



THE UNIVERSITY *of* EDINBURGH

Edinburgh Research Explorer

## Using multistage design-based methods to construct abundance indices and uncertainty measures for Delta Smelt

**Citation for published version:**

Polansky, L, Mitchell, L & Newman, K 2019, 'Using multistage design-based methods to construct abundance indices and uncertainty measures for Delta Smelt', *Transactions of the American Fisheries Society*, vol. 148, no. 4, pp. 710-724. <https://doi.org/10.1002/tafs.10166>

**Digital Object Identifier (DOI):**

[10.1002/tafs.10166](https://doi.org/10.1002/tafs.10166)

**Link:**

[Link to publication record in Edinburgh Research Explorer](#)

**Document Version:**

Peer reviewed version

**Published In:**

Transactions of the American Fisheries Society

**General rights**

Copyright for the publications made accessible via the Edinburgh Research Explorer is retained by the author(s) and / or other copyright owners and it is a condition of accessing these publications that users recognise and abide by the legal requirements associated with these rights.

**Take down policy**

The University of Edinburgh has made every reasonable effort to ensure that Edinburgh Research Explorer content complies with UK legislation. If you believe that the public display of this file breaches copyright please contact [openaccess@ed.ac.uk](mailto:openaccess@ed.ac.uk) providing details, and we will remove access to the work immediately and investigate your claim.



1 Using multistage design-based methods to construct abundance indices and uncertainty measures  
2 for Delta Smelt

3 Leo Polansky\*

4 Corresponding author

5 US Fish and Wildlife Service, Bay-Delta Field Office, Sacramento, CA, USA

6 leo.polansky@fws.gov

7

8 Lara Mitchell\*

9 US Fish and Wildlife Service, Lodi Fish and Wildlife Office, Lodi, CA, USA

10 lara\_mitchell@fws.gov

11

12 Ken B. Newman\*

13 US Fish and Wildlife Service, Lodi Fish and Wildlife Office, Lodi, CA, USA

14 Current affiliation: Biomathematics & Statistics Scotland and School of Mathematics, The Uni-  
15 versity of Edinburgh, Scotland, UK

16 ken.newman@bioss.ac.uk

17

18 \*All authors contributed equally.

19 RUNNING TITLE:

20 DELTA SMELT ABUNDANCE INDICES AND UNCERTAINTIES

21 *Abstract*

22 Population abundance indices and estimates of uncertainty are starting points for many scientific  
23 endeavors. However, if the indices are based on data collected by different monitoring programs  
24 with possibly different sampling procedures and efficiencies, applying consistent methodology for  
25 calculating them can be complicated. Ideally the methodology will provide indices and associ-  
26 ated measures of uncertainty that account for the sample design, the level of sampling effort (e.g.,  
27 sample size), and capture or detection probabilities. We develop and demonstrate such consistent  
28 methodology to multiple monitoring programs that sample different life stages of Delta Smelt, a  
29 critically endangered fish species endemic to the San Francisco Estuary whose abundance indices  
30 have been at the center of much controversy and debate given the regulatory consequences of their  
31 listed status. Current indices use different and incomparable methods, do not account for gear  
32 selectivity, and do not provide measures of uncertainty. Using recently available information on  
33 gear specific length-based conditional probabilities of capture given availability, we develop new  
34 abundance indices along with measures of uncertainty using a single methodological approach.  
35 These new indices are highly correlated with existing ones, but the approach applied here illumi-  
36 nates different sources of bias and quantifies between year variation using probabilistic statements  
37 where the previous indices cannot. Decomposition of uncertainty into constituent sources reveals  
38 that early life-stage uncertainty is dominated by gear inefficiency while later life-stage uncertainty  
39 is dominated by sample size, thus providing guidance for improvements to existing surveys. An  
40 additional result of general methodological interest is a demonstration, via simulation intended to  
41 reflect realistic data properties, that use of a lognormal distribution is to be preferred over the nor-  
42 mal distribution for making probabilistic statements about the indices. The work here facilitates  
43 the fitting of models attempting to identify factors associated with the dynamics and decline of the  
44 species.

## 45 <A> INTRODUCTION

46 Quantitative measures of life stage specific fish species abundances over time are important starting  
47 points for understanding life-history, assessing species status, and population modeling (e.g., stock  
48 synthesis). Fish monitoring programs provide the data for constructing such measures, referred to  
49 here as abundance indices. For status assessment and population modeling, abundance indices are  
50 used to identify relative or absolute abundance trends and drivers of population dynamics.

51 There are many approaches to deriving abundance indices, including design-based statistical ap-  
52 proaches (Thompson 2002), model-assisted design-based approaches (Maunder and Punt 2004),  
53 and model-based approaches, e.g., geospatial models (Thorson et al. 2015). Fundamentally, these  
54 approaches differ in their assumptions about the sources of variability in the data (Gregoire 1998).  
55 The approach taken for a given species depends on species biology, survey methodology, what  
56 methods of analysis are achievable given data limitations, and expectations about future applica-  
57 tions of the resulting indices. Although model-based approaches for survey data can accommodate  
58 greater spatial variation in densities between sites than design-based approaches (Thorson et al.  
59 2015), design-based approaches are often simpler, make fewer assumptions, can be constructed  
60 when data cannot support estimation of complex models, and can still be modified to account for  
61 processes such as gear selectivity (Newman 2008), reasons which motivate our choice of a design-  
62 based method here.

63 Regardless of the method used to calculate abundance indices, associated measurements of uncer-  
64 tainty about the indices are essential. First, they are necessary for determining whether apparent  
65 changes in abundance are significant according to some statistical criteria. Extending this concept  
66 to sampling, abundance indices can be described as true abundance multiplied by some bias factor  
67 plus additional sampling noise (page 60, Hilborn and Mangel 1997), and biologically implausible  
68 changes in abundance indices can point to changes in the bias parameter. Finally, measures of  
69 uncertainty can facilitate the fitting of population dynamics models to identify factors that impact

70 population vital rates (Knape et al. 2013; Newman et al. 2014).

71 A species currently lacking indices with uncertainty measures is Delta Smelt (*Hypomesus transpaci-*  
72 *ficus*), a small-bodied (adults are 50-90mm FL) Osmerid endemic to the upper “Delta” portion of  
73 the San Francisco Estuary (Moyle and Herbold 1992). Delta Smelt is a near annual species: spawn-  
74 ing occurs in late winter and early spring and individuals in the resulting cohort develop through  
75 several intermediate life-stages before maturing into the spawning life-stage by the subsequent  
76 winter (Bennett 2005). Delta Smelt monitoring has been ongoing since the late 1950s, although  
77 not until the mid 1990s were surveys specifically designed for Delta Smelt regularly deployed.

78 Abundance indices from the 1980s and early 1990s, including two California Department of Fish  
79 and Wildlife (CDFW) long-term fish monitoring programs, the Summer Towntnet (STN) and Fall  
80 Midwater Trawl (FMWT) surveys, indicated a precipitous decline during this time period (Moyle  
81 and Herbold 1992). In 1993, both the US Fish and Wildlife Service (USFWS) pursuant to the En-  
82 dangered Species Act of 1973 and the state of California under the California Endangered Species  
83 Act listed the species as threatened (CDFW 2010, USFWS 1993). Delta Smelt is currently one  
84 of the highest profile endangered fishes in the United States because their habitat coincides with a  
85 water supply that supports approximately 8 percent of the country’s population and a large agri-  
86 cultural economy, resulting in major resource conflicts between environmental and human needs  
87 (Delta Stewardship Council 2018). Despite these listings and an issuance of a 2008 biological  
88 opinion by the USFWS to mitigate impacts of water operations, Delta Smelt abundance indices in-  
89 dicate that the population size has continued to decline (Moyle et al. 2016; Polansky et al. 2018).  
90 In 2010 the state of California uplisted its status to endangered (CDFW 2010) under the Califor-  
91 nia Endangered Species Act, the USFWS warranted the uplisting of the species, and the species  
92 remains critically endangered according to the International Union for Conservation of Nature  
93 (NatureServe 2014).

94 The Delta Smelt abundance indices most frequently used for assessing trends and conducting pop-

95 ulation modeling have been derived by CDFW and use the 20-mm, STN, FMWT, and Spring  
96 Kodiak Trawl (SKT) surveys. Generally, these indices are sums of catch per unit effort (CPUE)  
97 calculated for different subregions of the Delta, with the level of spatial stratification and weighting  
98 of subregion water volumes varying between surveys. However, these indices do not have associ-  
99 ated measures of uncertainty and implicitly assume that the probability of catching Delta Smelt is a  
100 constant throughout the survey period. As such, it is difficult to make direct comparisons between  
101 the different survey indices to assess where bias correction factors may be needed in population  
102 modeling, and impossible to incorporate information about the uncertainties of the indices for trend  
103 analyses or modeling.

104 Here we develop a design-based method for calculating Delta Smelt abundance indices and as-  
105 sociated uncertainties that incorporates estimates of gear selectivity probabilities and assumptions  
106 about fish availability. The method is designed to be applied to data from multiple surveys, irre-  
107 spective of the type of fish sampling gear and deployment protocols used, to produce comparable  
108 abundance indices and measures of their uncertainty. We apply the method to Delta Smelt catch  
109 data from five surveys (20-mm, STN, FMWT, SMWT, and SKT) to generate abundance indices  
110 for four life stages of Delta Smelt: post-larval, juvenile, sub-adult, and adult. We use these results  
111 to assess recent changes in abundance and investigate potential biases in the data that lead to unre-  
112 alistic estimates of survival between life stages. Viewing the surveys as intrinsically a multistage  
113 sampling design (Hankin 1984; Newman 2008) enables us to quantify the relative contribution of  
114 different sources of variance, which provides insight into (1) features of abundance trends in recent  
115 years beyond clear multi-decadal changes, and (2) strategies for improved monitoring. Finally, we  
116 use simulations to test whether describing the abundance index distribution using a lognormal  
117 distribution, commonly applied in state-space population models (e.g., de Valpine and Hastings  
118 [2002]), is to be preferred over a normal distribution, the one that arises in large-sample theory  
119 descriptors of estimate distributions (Thompson 2002).

120 <A>METHODS

121 *Survey data.*— Delta Smelt abundance indices for four different life stages, post-larval, juvenile,  
122 sub-adult, and adult, were made using data collected by the five CDFW fish monitoring pro-  
123 grams mentioned previously. These surveys differ in terms of their duration, time of year sam-  
124 pled (thus life stage sampled), and sampling intensity (Table 1). For each survey the same sam-  
125 pling locations (sites) are visited each year (Figure S1). These locations were not randomly  
126 chosen, however, but were purposively selected with the aim of being geographically dispersed  
127 across the Delta (Chadwick 1964). All surveys are conducted by pulling nets of varying mesh  
128 sizes through the water behind or between boats, where the net mesh size decreases from the  
129 net opening to the closed tapered end (the cod end). The ordering of cod-end mesh size, from  
130 smallest to largest, for the surveys is 20-mm, STN, FMWT and SMWT (same as the FMWT),  
131 and SKT. The 20-mm and STN surveys, which usually make three tows at each sample site,  
132 use a rigid opening net that is dropped behind the boat, allowed to sink to varying depths and  
133 then gradually pulled to the surface as the boat moves forward. The FMWT and SMWT both  
134 use a midwater trawl, which has a 12 ft by 12 ft mouth opening held open by planing doors,  
135 that is dropped in the water, allowed to sink, and then gradually towed to the surface. The  
136 SKT uses two boats to pull a Kodiak trawl net through the water, slightly below and parallel to  
137 the surface. Further details on the surveys along with CDFW derived indices can be found at  
138 <https://www.wildlife.ca.gov/Conservation/Delta>.

139 For each survey, the samples taken at a given site include information on the spatial location, date,  
140 time of sampling, the number and lengths of Delta Smelt caught, and estimates of the volume of  
141 water sampled. Of relevance to the adjusted catch estimation procedure used in the index calcu-  
142 lations (see section “Sample catch adjustments”), the STN, FMWT, and SMWT surveys did not  
143 originally take length measurements nor record volume sampled, but over time this became rou-  
144 tine. Length measurements and volume calculations have always been made by the 20-mm and

145 SKT surveys. Partially due to the lack of length and volume measurements in earlier years, the  
146 abundance indices reported herein are for 1990 onward.

147 Several immediate observations are worth pointing out to contextualize the subsequent choices and  
148 assumptions of the method. The catch data at the survey-data-location resolution display frequen-  
149 cies of zero recorded catch ranging from 74% for the SKT survey to 92% for the FMWT survey  
150 with sometimes high spatial clustering in the regions where fish were caught. These observations  
151 motivated the use of a post-stratification (described in the next section) and pure design-based  
152 approach, rather than a spatial modeling approach.

153 Additional remarks about the 20-mm and STN surveys, which conduct repeated tows, is also nec-  
154 essary. To evaluate any evidence of fish depletion after the first tow, negative binomial regression  
155 models controlling for effort and with or without a tow effect between the first and second tow  
156 were compared using likelihood ratio test (LRTs). No evidence was found for either survey (20-  
157 mm LRT:  $\chi^2=0.14$ ,  $df=1$ ,  $p\text{-value}=0.71$ ; STN LRT:  $\chi^2=0.38$ ,  $df=1$ ,  $p\text{-value}=0.54$ ), supporting the  
158 assumption of catch independence across tows and an absence of any depletion effect.

159 *Geographic stratification and strata volume calculations.*– The design-based abundance indices  
160 that are calculated for different Delta Smelt life stages are in all cases stratified random ratio  
161 estimates, where the ratios are (gear-selectivity adjusted) catches divided by (adjusted) volume  
162 sampled that are then multiplied by estimates of stratum volumes. In this section we describe the  
163 stratification and in the next two sections discuss the sample catch and sample volume adjustments.

164 The Delta was partitioned into 29 subregions (Figure 1). The basis for the stratification was par-  
165 tially historical (being similar to the stratification used for some of the fish indices calculated by  
166 CDFW) and partially based on similar environmental conditions within a stratum. Additionally,  
167 post-stratification of the sampling locations into smaller geographic regions can lessen the amount  
168 of selection bias due to non-random selection of sampling locations.



169 For each stratum, the volume of water likely to be occupied by Delta Smelt was calculated from  
170 raster files describing the bathymetry of the Delta (Fregoso et al. 2017). Two sets of volume  
171 calculations were made, one for the volume between the surface and 10m depth, labeled the *early*  
172 *life stage volume*, and one for the volume between 0.5 and 4.5 depths, labeled the *later life stage*  
173 *volume* (Supplement Table S1). The early life stage volume was applied to the 20-mm survey  
174 catches and the later life stage volume was applied to all other surveys. The selection of volumes  
175 is somewhat speculative as definitive measurements of occupancy by depth are lacking. Support  
176 for the early life stage volume specification is largely based on Rockriver (2004), who found that  
177 younger fish appeared to be relatively evenly and deeply distributed throughout the water column.  
178 Support for juvenile and later life stages being more surface oriented are based on observations that  
179 surface tows done during the summer, fall, and winter result in higher catch densities compared  
180 with oblique tows done during the same seasons (Souza 2002; Mitchell et al. 2017).

181 *Sample catch adjustments.*— Fish capture probabilities can be viewed as a product of two proba-  
182 bilities, a (marginal) probability that a fish is present and initially available for capture by the gear  
183 and a conditional probability of catching or retaining the fish given that it is available to the gear  
184 (e.g., it is present in the volume of water passing through the net) (Crone et al. 2013). Including a  
185 length aspect to the retention probability, this probability can be expressed as  $\Pr(\text{Catch Fish}_L) =$   
186  $\Pr(\text{Fish}_L \text{ Available}) \times \Pr(\text{Caught}|\text{Fish}_L \text{ Available})$ , where  $\Pr(\text{Caught}|\text{Fish}_L \text{ Available})$  is contact  
187 selectivity (Crone et al. 2013), and each caught fish of length  $L$  represents  $1/\Pr(\text{Catch Fish}_L)$   
188 fish.

189 For the abundance index calculations made here, catches of fish in individual tows from each  
190 survey were upwardly adjusted using only estimates of gear-specific, length-based estimates of  
191 contact selectivity. If the probability of availability was exactly one for all fish present (per gear,  
192 sampling location and occasion), then such expansions could yield estimates of absolute abun-  
193 dance. However, this is almost certainly not true, and is one reason why the values constructed

194 here are labeled “indices” and not estimates of the true abundance.

195 Length-based, gear-specific contact selectivity functions were obtained from Mitchell et al. (2017)  
196 and Mitchell et al. (2019). In Mitchell et al. 2017, a cover was placed over the codend of the  
197 FMWT (and SMWT) gear and an assumption was made that all fish that slipped through the  
198 codend mesh were retained by the cover. In Mitchell et al. (2019), different combinations of 20-  
199 mm, STN, and SKT gear were deployed more or less simultaneously in the same area. In this  
200 case, because direct information on the length distribution of the population is not available, the  
201 estimated curves are relative selectivity curves (Millar and Fryer 1999). For practical purposes,  
202 relative selectivity means that the scaling of the selectivity functions cannot be determined, and is  
203 thus another reason for the label “index”.

204 Catch by a given gear  $g$  was adjusted as follows. Let  $c_{g,o}$  be the number of Delta Smelt caught by  
205 gear  $g$  on occasion  $o$  (where  $o$  denotes an arbitrary year, month, stratum, sampling location, and in  
206 the case of 20-mm and STN, an arbitrary tow). Let  $L_{g,o,i}$  be the length of the  $i^{\text{th}}$  fish in that catch  
207 and  $\hat{p}_g(L_{g,o,i})$  be an estimate of the contact selectivity probability for that fish (where  $p_g$  is a true  
208 but unknown function). The *adjusted catch*, denoted  $c_{g,o}^*$ , is

$$c_{g,o}^* = \sum_{i=1}^{c_{g,o}} \frac{1}{\hat{p}_g(L_{g,o,i})} \quad (1)$$

211 The range of fish lengths recorded in the catch data in some cases exceeded the range lengths used  
212 to estimate selectivity curves. For fish outside the range, we assigned captured probability values  
213 from the nearest endpoint of the curve.

214 *Sample volume adjustments.*– The volume of water towed during a survey often included portions  
215 of the water column assumed to be unoccupied by Delta Smelt, namely depths outside of the depths  
216 defined as early life stage volume or later life stage volume. *Effective volume*  $v^*$  was defined as the  
217 portion of a tow volume that intersected the relevant life stage stratum. The steps in the calculation

218 of effective volume are explained below.

219 The geometry of the effective volumes can be approximated by rectangular prisms, with oblique  
220 tows (used by 20-mm, STN, FMWT, and SMWT) described by non-right prisms and surface tows  
221 (used by SKT) described by right prisms. For oblique tows non-right prism volume is a function  
222 of tow depth and the net mouth height. Because tow depths were not routinely recorded, tow depth  
223 was estimated using the angle at which the trawl was deployed, the length of the cable released,  
224 and the block height (the height from the water surface to the block from which the cable is re-  
225 leased). Per survey protocols, an increase of 25 ft in the length of cable released corresponds to an  
226 approximately 1.2 m increase in the depth of the trawl. We used average block heights (calculated  
227 across different boats) of 2.53 m for 20-mm (T. Morris, CDFW, personal communication), 2.48  
228 m for STN (F. La Luz, CDFW, personal communication), and 2.03 m for FMWT and SMWT (S.  
229 Finstad, CDFW, personal communication). Given the estimated tow depth, measures of net mouth  
230 height, total sample volume, and the upper and lower bounds of the fish stratum, the effective vol-  
231 ume was calculated as the intersection of volume swept by the trawl and the volume occupied by  
232 the fish. For the SKT surface tows and right prism geometry, the effective volume calculation was  
233 simply the intersection of the rectangular prism parallel to the water surface (calculated from tow  
234 volume and net mouth height) and the vertical band between 0.5 m and 4.5 m:

$$235 \quad v_{SKT}^* = v_{SKT} \times \left( \frac{netHeight - 0.5}{netHeight} \right) = v_{SKT} \times \left( \frac{1.8 - 0.5}{1.8} \right) = v_{SKT} \times 0.722$$

236 where  $netHeight = 1.8m$  is the height of the net mouth.

237 *Abundance indices and variances.*— The equations for abundance indices parallel the following  
238 expression for the true abundance of life stage ( $ls$ ) fish during year  $y$  and month  $m$ ,  $N_{ls,y,m}$ :

$$239 \quad N_{ls,y,m} = \sum_h^H N_{ls,y,m,h} = \sum_h^H V_{ls,h} \delta_{ls,y,m,h} \quad (2)$$

240 where  $h$  denotes a given geographic stratum (and  $H$  is the total number of strata), and the stratum  
 241 abundances,  $N_{ls,y,m,h}$ , are products of (true) stratum specific densities  $\delta_{ls,y,m,h}$  and habitat water  
 242 volumes  $V_{ls,h}$ . The general form for the abundance indices for all life stages is a stratified ratio-of-  
 243 means estimator (Thompson 2002):

$$244 \quad I_{ls,y,m,g} = \sum_{h=1}^H I_{ls,y,m,g,h} = \sum_{h=1}^{29} V_{ls,h} \hat{\delta}_{ls,y,m,g,h} \quad (3)$$

246 with

$$247 \quad \hat{\delta}_{ls,y,m,g,h} = \frac{\sum_{j=1}^{n_{y,m,g,h}} c_{ls,y,m,g,h,j}^*}{\sum_{j=1}^{n_{y,m,g,h}} v_{y,m,g,h,j}^*}, \quad (4)$$

249 where  $n_{y,m,g,h}$  is the number of tows by gear  $g$  in a year-month-stratum,  $c^*$  is the adjusted catch  
 250 (equation 1), and  $v^*$  is the adjusted volume.

251 For each cohort, four different life stage abundance estimate, labeled post-larval, juvenile, sub-  
 252 adult, and adult, were calculated based on May 20-mm, July-August STN, October-November  
 253 FMWT, and February-March SMWT and SKT data, respectively (the Supplemental Material in-  
 254 cludes additional indices for other choices of months). When multi-month pooling was done,  
 255 primarily to increase the number of sampling locations, the indices ostensibly reflect some average  
 256 abundance over the sampling period that implicitly includes mortality or recruitment, though the  
 257 latter is thought negligible by the month of June. In some cases sampling periods for a given sur-  
 258 vey spanned two months, e.g., some sampling locations in the 20-mm ‘‘June’’ survey were actually  
 259 sampled in July. In these cases we assigned the label  $m$  based on the month in which most samples  
 260 were taken.

261 The variance of  $I_{ls,y,m,g}$  is the sum of the variances of the stratum-specific indices,  $I_{ls,y,m,g,h}$ :

$$262 \quad Var(I_{ls,y,m,g}) = \sum_{h=1}^{29} V_{ls,h}^2 Var(\hat{\delta}_{ls,y,m,g,h}) \quad (5)$$

263 If the fishing gear was 100% efficient, the variance of  $\hat{\delta}$  could be estimated using standard design-  
 264 based formulas for an estimated ratio (Thompson 2002) that account for between sample variation  
 265 in the ratio estimate of number of fish within a stratum. Because the true number of fish is in  
 266 fact being estimated at each location by imperfect gear, two more sources of variation need to  
 267 be accounted for, accomplished by using ideas of multistage sampling and use of the law of total  
 268 variance (Hankin 1984; Newman 2008; Thompson 2002). For each stratum-specific estimate, there  
 269 are three sources of variation: (1) between sample location variation in fish density (the ratio of  
 270 fish to volume), (2) the randomness in catching fish that are available to the gear, which for a fish  
 271 of length  $L$  occurs with probability  $p_g(L)$  (assuming 100% availability), and (3) uncertainty in the  
 272 estimated probabilities of fish capture  $\hat{p}_g$ . Abbreviating the estimated probability of capture of the  
 273  $i^{\text{th}}$  fish on the  $j^{\text{th}}$  tow in stratum  $h$  by  $\hat{p}_{j,i}$  (omitting notation identifying the gear and length specific  
 274 dependency of this probability), the estimated variance of  $I_{ls,y,m,g}$  is

$$275 \quad \widehat{\text{Var}}(I_{ls,y,m,g}) = \sum_{h=1}^{29} \frac{V_{ls,h}^2}{(\bar{v}_{ls,y,m,g,h}^*)^2} \times \quad (6a)$$

$$276 \quad \left( \frac{1}{n_{ls,y,m,g,h}^2} \sum_{j=1}^{n_{y,m,g,h}} \sum_{i=1}^{c_{ls,y,m,g,h,j}} \left[ \underbrace{\left( \frac{1 - \hat{p}_{j,i}}{(\hat{p}_{j,i})^2} \right)}_{\text{source 2}} + \underbrace{\frac{1}{\hat{p}_{j,i}^4} \widehat{\text{Var}}(\hat{p}_{j,i})}_{\text{source 3}} \right] + \underbrace{\frac{\hat{s}_{ls,y,m,g,h}^2}{n_{y,m,g,h}}}_{\text{source 1}} \right) \quad (6b)$$

278 where  $\bar{v}_{ls,y,m,g,h}^*$  is the mean effective tow volume within the stratum and  $s_{ls,y,m,g,h}^2$  is the within-  
 279 stratum, between tow variability in ratio estimates:

$$280 \quad \hat{s}_{ls,y,m,g,h}^2 = \frac{\sum_{j=1}^{n_{y,m,g,h}} \left( c_{ls,y,m,g,h,j}^* - \hat{\delta}_{ls,y,m,g,h} \times v_{y,m,g,h,j}^* \right)^2}{n_{y,m,g,h} - 1} \quad (7)$$

282 Details of the derivation are given in Appendix A, where the finite population correction factor is  
 283 assumed negligible (Thompson 2002). The estimated standard error  $\widehat{SE}_{ls,y,m,g}$  is the square root  
 284 of Equation 6, and the estimated coefficient of variation  $\widehat{CV}_{ls,y,m,g}$  is the ratio of the standard error

285 to the index.

286 Stratum-level variance estimates were undefined when there was only one sample taken and the  
287 median of the stratum specific values of Equation 6b was substituted. If the catch density was  
288 exactly the same across all sites (practically if a stratum had 0 total catch), the variance contribution  
289 for that stratum was set to 0.

290 *Abundance indices with truncated contact selectivity functions.*— A practical problem when adjust-  
291 ing catch using capture probabilities is that very small values of  $\hat{p}_g(L)$  can lead to unrealistically  
292 large adjusted catch values. This was of particular concern for the non-monotonic 20-mm and STN  
293 selectivity curves identified by the data, which were not informed by many captures of large fish  
294 (Mitchell et al. 2019). To investigate the effects of this problem, we compared indices based on  
295 the original selectivity curves to estimates based on “truncated” curves, defined to be the same as  
296 the original curves except with the descending tail of each curve replaced by a horizontal line at  
297 one (see Figure 7 in Mitchell et al. 2019).

298 *Measures of vital rates.*— Abundance indices for successive life stages were used as measures of  
299 vital rate parameters such as recruitment (number of young produced per adult) and between life  
300 stage survival for given cohorts. Such measures are calculated by taking ratios of indices for  
301 successive life stages. For example, an approximate measure of the recruitment of post-larvae  
302 ( $pl$ ) in cohort  $t + 1$  from adults ( $a$ ) in cohort  $t$  is  $I_{t+1,pl}/I_{t,a}$ . Similarly, a relative measure of  
303 survival of juveniles ( $j$ ) to sub-adults ( $sa$ ) is  $I_{t,sa}/I_{t,j}$ . Being indices and not unbiased estimates of  
304 absolute abundance, such ratios are unlikely to provide estimates of actual recruitment or survival  
305 rates, but may allow population growth rate estimates  $I_{t+1,a}/I_{t,a}$  if all unknown scaling factors and  
306 availability probabilities are constant in time because they will cancel out.

307 *Decomposition of variance components.*— The three sources of variation making up the index vari-  
308 ance estimate shown in Equation 6 can be multiplied out so that the variance is the sum of terms  
309 corresponding to each source separately, i.e.,  $\widehat{\text{Var}}(I_{l,s,y,m,g}) = s_1 + s_2 + s_3$  where  $s_i$  is the  $i^{\text{th}}$

310 source of variance (the life stage, time and gear specific indices on the right hand side have been  
311 suppressed for clarity). For each index, we computed the fraction of its total variance by source  
312  $i$ ,  $f_i = s_i / (s_1 + s_2 + s_3)$  to describe how these changed across life stages and within life stages  
313 across years.

314 *Lognormal distribution-based confidence intervals and a simulation study.*— One approach for con-  
315 structing  $\alpha$ -level confidence intervals for the indices is to assume that the estimated indices are  
316 approximately normally distributed and set the interval equal to  $I \pm z_{1-\alpha/2} \sqrt{\widehat{V}(I)}$ , where  $z_{1-\alpha/2}$   
317 is the  $1-\alpha/2$  quantile of a standard normal distribution. Justification for the normality assumption  
318 (the Central Limit Theorem) when sampling from a finite population without replacement is more  
319 complicated (Thompson 2002), but tows can reasonably be viewed as sampling with replacement  
320 given the extremely small sample volumes relative to the potential habitat volumes (Table S2).  
321 More critically, a practical problem with quantities like indices, which have to be non-negative, is  
322 that such intervals can have negative lower bounds; e.g., a 95% interval will have a negative lower  
323 bound when the coefficient of variation of the estimate exceeds 0.51.

324 Here we used an alternative approach that assures intervals above zero by assuming the indices are  
325 lognormally distributed. Dropping the  $ls$ ,  $y$ ,  $m$ , and  $g$  subscripts, the parameters of the lognormal  
326 distribution are the log-mean  $\mu = \ln \left( I / \sqrt{1 + \widehat{CV}^2} \right)$  and  $\sigma^2 = \ln \left( 1 + \widehat{CV}^2 \right)$ , which as con-  
327 structed ensures that the expected value of the distribution is the index  $I_{ls,y,m,g}$ . Then given an  $\alpha$ ,  
328 the confidence interval is given by the  $\alpha$  and  $1 - \alpha$  quantiles of this lognormal distribution.

329 A simulation experiment (described in detail in Supplement E) was designed to gain insight into  
330 the performance of the estimation procedure and the use of the lognormal distribution as described  
331 above for constructing confidence intervals given a multistage data generation process. Nine dif-  
332 ferent selectivity curves were used in combination with realistic sample sizes (i.e., very small).  
333 The data generating process used a baseline abundance,  $N_{Tot}$ , of 102,000 fish, corresponding to  
334 a stratum level density of 1 fish per 10,000m<sup>3</sup> of habitat, all available to be sampled. Potential

335 catch was then simulated according to a negative binomial model, and a logistic contact selectivity  
336 selectivity curve was used to simulate a realized catch. Variation in numbers caught was purely  
337 a function of between sample catch variation and contact selectivity, as availability was assumed  
338 to be 100%; thus, in this case, the estimated totals  $\hat{N}_{Tot}$  are of the simulated baseline abundance  
339 value. A total of 1,000 simulations for each choice of gear selectivity curves were made. Bias  
340 (relative to the simulated baseline abundance) and standard errors of  $\hat{N}_{Tot}$  were recorded, and the  
341 actual coverage of lognormal-based confidence intervals was compared to the nominal coverage of  
342 95% and contrasted with normal distribution-based intervals.

## 343 <A>RESULTS

344 <B> *Sample catch adjustments.*— By design, adjusted catches are always greater than or equal to  
345 the corresponding non-adjusted catches, leading to catch inflation factors (adjusted catch divided  
346 by non-adjusted catch) that are greater than or equal to one. For 20-mm catches, the mean inflation  
347 factor was 5.05 (SD, 6.12), ranging from 1.00 to 22.49. For STN catches, the mean inflation factor  
348 was 1.70 (SD, 1.41), ranging from 1.0 to 44.01. For FMWT catches, the mean inflation factor  
349 was 3.18 (SD, 0.75), ranging from 1.00 to 4.35. For the SMWT, the mean inflation factor was  
350 1.78 (SD, 0.59), ranging from 1.0 to 3.91. Adjusted SKT catches were identical to non-adjusted  
351 catches because the estimated relative selectivity of the SKT gear was one over the range of lengths  
352 observed.

353 <B> *Sample volume adjustments.*— Effective sample volumes were always less than or equal to  
354 the corresponding raw sample volumes. For the 20-mm survey, effective and raw volumes were  
355 identical. For the STN survey, effective volumes were generally smaller than raw volumes, with a  
356 mean factor of 0.71 (SD, 0.17), ranging from 0.53 to 0.97. For the FMWT survey, the mean factor  
357 was 0.78 (SD, 0.10), ranging from 0.66 to 0.96. For SMWT, the mean factor was 0.78 (SD, 0.09),  
358 ranging from 0.66 to 0.96.

359 <B> *Abundance indices and variances.*— Declines over the past several decades in Delta Smelt



360 abundances across all life stages as measured by the indices is clearly evident (Table 2 and Figure  
361 2). The uncertainties in the indices, as measured by the CVs, were on average 37.04%, 33.59%,  
362 45.51%, 24.33%, and 30.90% for the 20-mm, STN, FMWT, SMWT, and SKT-based indices, re-  
363 spectively. These abundance indices are highly correlated with the corresponding CDFW indices  
364 for the years in which both are estimated (Figure 3). Both show similar long-term downward  
365 trends and localized periods of relatively high and low values, and with a few exceptions track  
366 the year-over-year changes (increases or decreases). Notable differences include indices of post-  
367 larvae based on the 20-mm survey data where the new indices indicate higher recruitment success  
368 for 1996 and lower recruitment success for 1999 relative to CDFW indices.

369 Very recent (2013-2017) adult abundance indices have also showed a decline. The upper confi-  
370 dence intervals in the years 2016 and 2017 are lower than the lower confidence intervals for the  
371 years 2013-2015, suggesting a continued downward trend in recent years (Figure 4). In particular,  
372 the decline after 2015 reflects a record low population growth rate of 0.13 for the 2015 cohort.

373 <B> *Abundance indices with truncated contact selectivity functions.*— The indices based on trun-  
374 cated contact selectivity curves results can be considerably smaller (Supplement F and Figure S4).  
375 For the 20-mm survey, non-truncated point indices ranged from about one to two (June data) or 10  
376 (July data) times larger than the truncated indices, while for the STN survey, non-truncated indices  
377 were between one and two times greater than truncated indices for STN survey (Table S8). The  
378 non-truncated and truncated indices are highly correlated (Table S9 and Figure S4). As expected,  
379 the proportion of variance of an abundance index from catch randomness decreased when truncated  
380 selectivity curves were used to adjust catch (Figure S5).

381 <B> *Measures of vital rates.*— Estimates of (relative) recruitment (post-larvae per adult) are re-  
382 ported separately for the 1995-2001 adults and later adults because of a likely change in the adult  
383 abundance index bias from 2001 to 2002 when the adult sampling gear changed from a midwater  
384 trawl (the SMWT survey) to a Kodiak trawl (the SKT survey). Mean estimated recruitment for

385 cohorts in the earlier period is 89.07 post-larvae per adult (SD, 74.43), ranging from a minimum  
386 of 38.80 per adult in 1998 to 248.20 per adult in 1997. Mean estimated recruitment for cohorts in  
387 the later period is 14.66 post-larvae per adult (SD, 9.82), ranging from a minimum of 3.24 in 2015  
388 to a maximum of 41.72 in 2005.

389 Post-larval survival rates ranged from a minimum of 0.01 juveniles per post-larva in 2015 to a  
390 maximum plausible value of 0.85 juveniles per post-larva in 2011, and a single larger, and implau-  
391 sible ( $>1.0$ ), value. Juvenile survival rates range from a minimum of 0.01 sub-adults per juvenile  
392 in 1996 to a maximum plausible value of 0.90 in 2015, and a single value larger than 1. Sub-adult  
393 survival rate estimates were especially problematic, with 13 of the 16 based on SKT adult abun-  
394 dances being larger than 1. Given that the SMWT and FMWT used identical gear, the unmeasured  
395 gear efficiencies (e.g., related to availability to the gear) are presumably quite similar, thus gear-  
396 selectivity effects when comparing these estimates should be minimal. For the subset of sub-adult  
397 survival rates based on SMWT adult indice estimates (11 total), plausible values range from 0.09  
398 adults per sub-adult in 1991 to 0.52 in 1998, with two being implausibly large ( $>1$ ).

399 Cohort population growth rates, each the product of the post-larval recruitment value and the three  
400 survival rates of the subsequent life stages, ranged from 0.13 in 1996 to 9.50 in 1995 for the cohorts  
401 with adult abundance indices measured with the SMWT survey, and from 0.13 in 2015 to 4.74 in  
402 2011 for the cohorts with adult abundance indices measured with the SKT survey. The 2012  
403 adult abundance index is noticeably higher than other contemporary abundance indices, likely a  
404 reflection of the relatively large population growth rate in 2011, the next largest being 1.42 in 2016  
405 when abundances were relatively very low.

406 **<B>** *Decomposition of variance components.*— The proportion of variance contributed by each  
407 of the three separate sources of variability depended on the combination of gear and life stage  
408 (Figure 5). The variance of the 20-mm survey based index is slightly dominated by the randomness  
409 in catching fish that are available to the gear (source 2), followed by between sample location

410 variability in fish density (source 1), with relatively little contribution from the uncertainty in the  
411 estimated probabilities of fish capture (source 3). In contrast, the sources of STN, FMWT, SMWT,  
412 and SKT abundance index uncertainties are all dominated by source 1 variability.

413 <B> *Lognormal distribution-based confidence intervals and the simulation study.*— The simulation  
414 study showed that the distributions of the multi-stage estimates of abundance are right-skewed,  
415 with the degree of skewness varying as a function of the contact selectivity parameters (Figure  
416 S3). The estimates  $\hat{N}_{Tot}$  have relatively small bias even for highly inefficient gear, ranging from  
417 -1% to 2% (Table S5). However, the average coefficient of variation (for indices with non-zero  
418 values) range from 37% to 91% (Table S6). Such CVs, while relatively large, are within the range  
419 of the empirical estimates from the Delta Smelt dataset (Figure 2). Baseline abundance estimates  
420  $\hat{N}_{Tot}$  equal to zero resulted only when using the selectivity curves with near zero values across  
421 much of the range of fish lengths (Table S7).

422 Actual coverage of the 95% confidence intervals based on the lognormal distribution is affected  
423 by the contact selectivity function. For the logit models corresponding to overall intermediate se-  
424 lectivity ( $\beta_0=0.5$ ), observed coverage equaled nominal coverage. However, with the overall high  
425 selectivity models ( $\beta_0 = -0.5$ ), observed coverage was slightly low (from 90% to 94%), while for  
426 the overall low selectivity models ( $\beta_0=0.9$ ) coverage was too high (from 97% to 100%). Confi-  
427 dence intervals based on a normal distribution, which were also affected by the contact selectivity  
428 curves, increasingly yielded negative lower bounds as  $\beta_0$  increased, from up to 4% with  $\beta_0 = -0.5$ ,  
429 20% to 26% with  $\beta_0 = 0.5$ , and up to 100% with  $\beta_0 = 0.9$ .

## 430 <A> **DISCUSSION**

431 A single, well-established finite population sample estimation procedure, namely, stratified random  
432 sample ratio expansions (Thompson 2002), was applied to trawl catch data collected from several  
433 long-term fish monitoring programs to calculate survey-specific point estimates of relative abun-  
434 dance along with variances. These abundance indices are strongly correlated with the conventional

435 indices, with both showing substantial declines over the past several decades. Because a similar  
436 estimation procedure was applied to all the surveys, direct comparisons of estimates between sur-  
437 veys were possible, identifying that at least the FMWT and SMWT survey indices continue to be  
438 relatively biased compared with other indices, despite corrections for gear selectivity. This sort  
439 of bias identification can be useful for population modeling efforts, particularly for structuring the  
440 observation error equations.

441 The uncertainty measures, variances, and confidence intervals, provided insights beyond those  
442 possible from point estimates alone. Firstly, in conjunction with the lognormal assumption about  
443 the point estimate distribution, it appears that abundances in the past few years have continued to  
444 decline significantly, something the conventional indices could not establish given the absence of  
445 estimates of uncertainty. The ability to make probabilistic statements about year over year changes  
446 in abundance is critical for scientific assessments about the changing status of the population.

447 Secondly, partitioning the variation into three categories helps identify how different life stages  
448 may be distributed throughout their habitat relative to the surveys. If there are many post-larval  
449 Delta Smelt for the 20-mm survey gear to encounter, then gear-related uncertainty overshadows  
450 between sample variability. One explanation for the apparent increase in the relative importance  
451 of between sample uncertainty from the post-larval to adult life stage is the inherent decline in  
452 population size from one life stage to the next. As the number of Delta Smelt available to each  
453 successive survey (STN, FMWT, then SMWT or SKT) decreases, patchiness of their distribution  
454 could increase, and between sample location variability becomes more important. The very high  
455 frequency of zero catch combined with sometimes very high catch totals could be evidence for  
456 such patchiness.

457 Thirdly, partitioning the variance also provides suggestions for both what is working and how im-  
458 provements in data collection procedures can be made. For the 20-mm survey, the largest compo-  
459 nent of variance came from randomness that a fish in the path of the gear will be caught, supporting

460 the multiple tows at a single location sample design, as is currently done. The relative dominance  
461 of between sample location variability for the STN, FMWT, SMWT, and SKT abundance indices  
462 suggests expanding spatial coverage for these surveys. Such an expansion of spatial coverage is a  
463 feature of a new enhanced Delta Smelt monitoring program conducted by the USFWS which sam-  
464 ples from an increased number of spatially random sites per stratum, and to date has consistently  
465 detected Delta Smelt when FMWT has not.

466 One gap in knowledge that potentially affects the quality of the abundance index estimates is  
467 poor understanding of precisely how Delta Smelt are distributed in the water column vertically  
468 and horizontally, and how this in turn might vary geographically across the strata. Despite the  
469 extensive monitoring, the percentage of total potential habitat sampled by a survey in a given month  
470 was typically much less than 1% (Table S2), limiting the ability to infer in detail the distribution  
471 of density. Spatial distribution affects how effective sample volumes should be calculated for  
472 estimating fish density within a stratum as well as how the stratum water volumes used for density  
473 expansions should be calculated (and ultimately affects the probability that fish are available to  
474 the gear). Evidence that fish availability to sampling gear depends on spatiotemporally dynamic  
475 habitat characteristics, particularly tide (Feyrer et al. 2013; Bennett and Burau 2015; Polansky et  
476 al. 2018) and turbidity (Feyrer et al. 2007; Nobriga et al. 2008; Polansky et al. 2018), further  
477 complicates the problem of identifying what portion of the potential habitat is actually occupied at  
478 any given moment.

479 How Delta Smelt are spatially distributed also has implications for whether catch densities should  
480 be further adjusted because a given survey may disproportionately sample from higher or lower  
481 density portions (both vertically and horizontally) of the habitat. While density estimates can be  
482 corrected to account for biased sampling, without the precise knowledge of spatial distributions  
483 any such corrections are assumption laden. However, spatial post-stratification of survey data can  
484 ameliorate some of the large-scale consequences of spatial density variation when expanding local

485 catch densities.

486 Another issue affecting the quality of the abundance indices is that none of the sampling locations  
487 visited here were randomly selected. The sites were instead purposively selected, with the same  
488 sampling locations visited over time, both within and between years, an *always revisit* monitoring  
489 design (McDonald 2012). In fact, the surveys share many of the same sampling locations, many  
490 of which were selected when the earliest survey, the STN survey, was originally established in the  
491 late 1950s and the (Fall and Spring) MWT survey was established in 1967. Thus in principle, the  
492 failure to randomly choose sampling locations could result in selection bias; e.g., if the sites were  
493 selected because of a priori knowledge that fish were more likely to be present. Further, because  
494 the chosen sites were located where the trawl gear could be safely and practically deployed, near-  
495 shore portions of the Delta volume are systematically excluded from the sample frame. This, in  
496 turn, could bias (high or low) indices if Delta Smelt densities change systematically in these areas,  
497 although the fraction of total habitat these areas represent is small.

498 Two factors that may partially alleviate the lack of randomness in the sample site selection are  
499 tidal dynamics of the Delta and spatial post-stratification. The spatiotemporal distribution of Delta  
500 Smelt is strongly affected by the tides (Bennett and Burau 2015). The volume of water at the same  
501 fixed location is a constantly changing volume of water, and pelagic fish, particularly relatively  
502 small fish like Delta Smelt, are thought to be constantly changing position, in some cases voli-  
503 tionally and in other cases due to hydrodynamics. Thus if one did continuously sample at a fixed  
504 geographic location throughout a single day, one is sampling a body of water that covers several  
505 kilometers (Bennett and Burau 2015). Spatial post-stratification can help also in that sampling  
506 locations purposively selected because they were thought to have relatively high fish densities will  
507 have less effect on estimated totals as the densities for such locations only affect the strata they are  
508 located in.

509 A somewhat more complicated situation is if gear deployment elicits a behavioral response by the

510 fish, causing them to either disperse or aggregate. For example, when nets are dragged behind  
511 boats, if the boat displaces the fish below it, that would cause an immediate change in availability  
512 that is not easily measured with the available trawl data alone. Alternatively, the use of two boats  
513 in the deployment of the Kodiak trawl in the SKT survey could act to herd the fish toward the  
514 net. One cannot say that the probability of availability is now greater than one (meaningless) but  
515 rather the volume sampled has in fact increased. There is some evidence for such herding from  
516 the gear evaluation studies as the two boat surface tow method used by SKT generally resulted in  
517 larger catch densities than the single boat oblique method used by the STN and FMWT surveys  
518 (Mitchell et al. 2017; Mitchell et al. 2019). More generally, features of how the nets are deployed  
519 in the water, such as position relative to the boat(s), speed, duration, and direction (relative to the  
520 direction the fish are swimming), have the potential to affect the relationship between water volume  
521 sampled and catch, and that relationship can be affected by local habitat features such as turbidity,  
522 temperature, and flow.

523 Another caveat is that the estimated length-based contact selectivity functions, the  $\hat{p}_q(L)$  (Mitchell  
524 et al. 2017; Mitchell et al. 2019) may be biased and inadequate. Skepticism about the ascending  
525 and descending limbs of dome-shaped selectivity curves led to the sensitivity analysis using the  
526 truncated curves and the effects on resulting abundance indices were sizable, e.g., up to a 10-  
527 fold decrease from non-truncated to truncated estimates. Equally critical is the fact that contact  
528 selectivity is undoubtedly a function of more than fish length alone. Polansky et al. (2018) showed  
529 that using a Poisson distribution for Delta Smelt catches, which implicitly assumes completely  
530 random spatial distributions, is inferior to the negative binomial distribution, which can reflect  
531 spatial aggregation (“patchiness”). If the probability of capture (for a fish that was available)  
532 was affected by the presence of other fish, then the underlying independence assumption of the  
533 contact selectivity model is violated, which further complicates fitting and applying such selectivity  
534 models.

535 In conclusion, despite these challenges and the observation that the indices constructed reveal the  
536 same temporal trend as the CDFW derived ones, constructing indices and associated uncertain-  
537 ties using a uniformly applied method was useful in several ways. Estimates of uncertainty and  
538 the simulation study (designed to identify how to incorporate this uncertainty into trend analysis)  
539 allowed further progress into understanding trends and biases, as well as recommendations for im-  
540 proved survey designs. Further, the work here can be used to guide life cycle model formulation  
541 and the resulting abundance indices and standard errors can serve as input data for fitting such  
542 models, which can in turn be used to help identify factors associated with the population dynamics  
543 and overall decline.

#### 544 <A> **ACKNOWLEDGMENTS**

545 We thank CDFW staff and Randy Baxter in particular for discussions on the topics written about  
546 here. Matt Nobriga, Will Smith, Vanessa Tobias, the Editor, the Associate Editor, and several  
547 anonymous reviewers provided helpful comments on an earlier version of this paper. The Califor-  
548 nia Department of Water Resources and the Interagency Ecological Program provided funding and  
549 permits for this work. The findings and conclusions in this article are those of the authors and do  
550 not necessarily represent the view of the member agencies of the Interagency Ecological Program  
551 for the San Francisco Estuary.

552

#### 553 <A> **REFERENCES**

554 Bennett, W. A. 2005. Critical assessment of the Delta Smelt population in the San Francisco  
555 Estuary, California. *San Francisco Estuary and Watershed Science* 3(2). Available: <https://escholarship.org/uc/item/0725n5vk>. (November 2018).

557 Bennett, W. A., and J. R. Burau. 2015. Riders on the storm: selective tidal movements facilitate the  
558 spawning migration of threatened Delta Smelt in the San Francisco Estuary. *Estuaries and Coasts*



559 38:826 835. (November 2018).

560 California Department of Fish and Wildlife (CDFW). 2010. Threatened and Endangered Fish.  
561 Available: [http://www.dfg.ca.gov/wildlife/nongame/t\\_e\\_spp/fish.html](http://www.dfg.ca.gov/wildlife/nongame/t_e_spp/fish.html). (Novem-  
562 ber 2018).

563 Chadwick, H. K. 1964. Annual abundance of young striped bass, *Roccus saxatilis*, in the Sacramento-  
564 San Joaquin Delta, California, California Fish and Game Bulletin. California Department of Fish  
565 and Game. Available: [http://www.dfg.ca.gov/delta/data/townet/bibliography.](http://www.dfg.ca.gov/delta/data/townet/bibliography.asp)  
566 asp. (February 2019).

567 Crone, P., M. Maunder, J. Valero, J. McDaniel, and B. Semmens. 2013. Selectivity: theory,  
568 estimation, and application in fishery stock recruitment models. Center for the Advancement of  
569 Population Assessment Methodology Workshop Series Report 1. Available: [https://swfsc.](https://swfsc.noaa.gov/publications/CR/2013/2013Crone.pdf)  
570 [noaa.gov/publications/CR/2013/2013Crone.pdf](https://swfsc.noaa.gov/publications/CR/2013/2013Crone.pdf). (November 2018).

571 Delta Stewardship Council. 2018. The Delta Plan: ensuring a reliable water supply for California,  
572 a healthy Delta ecosystem, and a place of enduring value. Available: [http://deltacouncil.](http://deltacouncil.ca.gov/delta-plan-0)  
573 [ca.gov/delta-plan-0](http://deltacouncil.ca.gov/delta-plan-0). (December 2018).

574 de Valpine, P. and A. Hastings. 2002. Fitting population models incorporating process noise and  
575 observation error. *Ecological Monographs* 72:57-76. Available: [https://www.jstor.org/  
576 stable/3100085](https://www.jstor.org/stable/3100085). (February 2019).

577 Feyrer, F., M. L. Nobriga, and T. R. Sommer. 2007. Multidecadal trends for three declining fish  
578 species: habitat patterns and mechanisms in the San Francisco Estuary, California, USA. *Canadian*  
579 *Journal of Fisheries and Aquatic Sciences* 64:723-734. Available: [https://doi.org/10.](https://doi.org/10.1139/f07-048)  
580 [1139/f07-048](https://doi.org/10.1139/f07-048). (February 2019).

581 Feyrer, F., D. Portz, D. Odum, K. B. Newman, T. Sommer, D. Contreras, R. Baxter, S. B. Slater, D.  
582 Sereno, and E. Van Nieuwenhuysse. 2013. SmeltCam: underwater video codend for trawled nets

583 with an application to the distribution of the imperiled Delta Smelt. PLoS ONE 8:e67829. Avail-  
584 able: <https://journals.plos.org/plosone/article?id=10.1371/journal.pone.0067829>. (November 2018).

586 Fregoso, T. A., R-F Wang, E. Alteljevich, and B. E. Jaffee. 2017. San Francisco Bay-Delta bathy-  
587 metric/topographic digital elevation model (DEM). U.S. Geological Survey, Coastal and Marine  
588 Geology Program. Available: <https://doi.org/10.5066/F7GH9G27>. (November 2018).

589 Gregoire, T.G. 1998. Design-based and model-based inference in survey sampling: appreciating  
590 the difference. *Canadian Journal of Fisheries and Aquatic Sciences* 28:1429-1447. Available:  
591 <https://doi.org/10.1139/x98-166>. (February 2019).

592 Hankin, D. G. 1984. Multistage sampling designs in fisheries research: applications in small  
593 streams. *Canadian Journal of Fisheries and Aquatic Sciences* 41:1575-1591. Available: <https://doi.org/10.1139/f84-196>. (February 2019).

595 Knape, J., P. Besbeas, and P. de Valpine. 2013. Using uncertainty estimates in analyses of  
596 population time series. *Ecology* 94:2097-2107. Available: <https://doi.org/10.1890/12-0712.1>. (February 2019).

598 Hilborn, R. and M. Mangel. 1997. *The Ecological Detective: confronting models with data*.  
599 *Monographs in Population Biology* 28. Princeton University Press. Princeton, NJ.

600 Maunder, M. N. and A. E. Punt. 2004. Standardizing catch and effort data: a review of recent  
601 approaches. *Fisheries Research* 70:141-159. Available: <https://doi.org/10.1016/j.fishres.2004.08.002>. (February 2019).

603 McDonald, T. 2012. Spatial sampling designs for long-term ecological monitoring. Pages 101-125  
604 *in* R. A. Gitzen, J. J. Millspough, A. B. Cooper, and D. S. Licht, editors. *Design and Analysis of*  
605 *Long-term Ecological Monitoring Studies*. Cambridge University Press, New York, NY.

606 Millar, R. B. and R. J. Fryer. 1999. Estimating the size-selection curves of towed gears, traps, nets,  
607 and hooks. *Reviews in Fish Biology and Fisheries* 9:89-116. Available: [https://doi.org/](https://doi.org/10.1023/A:1008838220001)  
608 [10.1023/A:1008838220001](https://doi.org/10.1023/A:1008838220001). (February 2019).

609 Mitchell, L., K. Newman, and R. Baxter. 2017. A covered cod-end and tow-path evaluation of mid-  
610 water trawl gear efficiency for catching Delta Smelt (*Hypomesus transpacificus*). *San Francisco*  
611 *Estuary and Watershed Science* 15(4). Available: [https://doi.org/10.15447/sfews.](https://doi.org/10.15447/sfews.2017v15iss4art3)  
612 [2017v15iss4art3](https://doi.org/10.15447/sfews.2017v15iss4art3). (November 2018).

613 Mitchell, L., K. Newman, and R. Baxter. 2019. Estimating the size selectivity of fishing trawls for  
614 short-lived fish species. *San Francisco Estuary and Watershed Science* 17(1). Available: [https://doi.org/10.15447/sfews.](https://doi.org/10.15447/sfews.2018v17iss1art5)  
615 [2018v17iss1art5](https://doi.org/10.15447/sfews.2018v17iss1art5)

616 Moyle, P. B., L. R. Brown, J. R. Durand, and J. A. Hobbs. 2016. Delta Smelt: life history  
617 and decline of a once-abundant species in the San Francisco Estuary. *San Francisco Estuary and*  
618 *Watershed Science* 4(2). Available: [https://escholarship.org/uc/item/09k9f76s.](https://escholarship.org/uc/item/09k9f76s)  
619 (November 2018).

620 Moyle, P. B. and B. Herbold. 1992. Life history and status of Delta Smelt in the Sacramento-San  
621 Joaquin Estuary, California. *Transactions of the American Fisheries Society* 121:67-77. Available:  
622 [https://doi.org/10.1577/1548-8659\(1992\)121<0067:LHASOD>2.3.CO;2](https://doi.org/10.1577/1548-8659(1992)121<0067:LHASOD>2.3.CO;2). (Febru-  
623 ary 2019).

624 NatureServe. 2014. *Hypomesus transpacificus*. The IUCN Red List of Threatened Species 2014:  
625 [e.T10722A18229095](http://dx.doi.org/10.2305/IUCN.UK.2014-3.RLTS.T10722A1822909). <http://dx.doi.org/10.2305/IUCN.UK.2014-3.RLTS.T10722A1822909>  
626 [en](http://dx.doi.org/10.2305/IUCN.UK.2014-3.RLTS.T10722A1822909). (November 2018).

627 Newman, K. B. 2008. Sample design-based methodology for estimating Delta Smelt abundance.  
628 *San Francisco Estuary and Watershed Science* 6(3). Available: [http://escholarship.](http://escholarship.org/uc/item/99p428z6)  
629 [org/uc/item/99p428z6](http://escholarship.org/uc/item/99p428z6) (November 2018).

630 Newman, K. B., S. T. Buckland, B. J. T. Morgan, R. King, D. L. Borchers, D. J. Cole, P. Besbeas,  
631 O. Gimenez, and L. Thomas. 2014. Modelling Population Dynamics. Methods in Statistical  
632 Ecology. Springer, New York, NY.

633 Nobriga, M. L., T. R. Sommer, F. Feyrer, and K. Fleming. 2008. Long-term trends in summer-  
634 time habitat suitability for Delta Smelt (*Hypomesus transpacificus*). San Francisco Estuary and  
635 Watershed Science 6. Available: <https://escholarship.org/uc/item/5xd3q8tx>.  
636 (November 2018).

637 Polansky, L., K. B. Newman, M. L. Nobriga, and L. Mitchell. 2018. Spatiotemporal Models  
638 of an Estuarine Fish Species to Identify Patterns and Factors Impacting Their Distribution and  
639 Abundance. Estuaries and Coasts 41:572-581. Available: [https://doi.org/10.1007/  
640 s12237-017-0277-3](https://doi.org/10.1007/s12237-017-0277-3). (February 2019).

641 Rockriver, A. 2004. Vertical distribution of larval Delta Smelt and Striped Bass near the conflu-  
642 ence of the Sacramento and San Joaquin rivers. Pages 97–109 in F. Feyrer, L. R. Brown, R. L.  
643 Brown, J.J. Orsi, editors. Early life history of fishes in the San Francisco Estuary and watershed.  
644 Symposium 39. Bethesda (MD): American Fisheries Society.

645 Souza, K. 2002. Revision of California Department of Fish and Game’s Spring Midwater Trawl  
646 and results of the 2002 Spring Kodiak trawl. Interagency Ecological Program for the Sacramento-  
647 San Joaquin Estuary Newsletter 15(3):44-47. Available: [https://www.wildlife.ca.gov/  
648 Conservation/Delta/Spring-Kodiak-Trawl/Bibliography](https://www.wildlife.ca.gov/Conservation/Delta/Spring-Kodiak-Trawl/Bibliography). (February 2019).

649 Thompson, S. K. 2002. Sampling. 2nd edition. Wiley Series in Probability and Statistics, John  
650 Wiley and Sons, Inc., New York, NY.

651 Thorson, J. T., A. O. Shelton, E. J. Ward, and H. J. Skaug. 2015. Geostatistical delta-generalized  
652 linear mixed models improve precision for estimated abundance indices for West Coast ground-  
653 fishes. ICES Journal of Marine Science 72:1297-1310. Available: <https://doi.org/10.>

654 1093/icesjms/fsu243. (February 2019).

655 U.S. Fish and Wildlife Service. 1993. Endangered and threatened wildlife and plants; determina-  
656 tion of threatened status for the Delta Smelt. Federal Register 58:12854-12864.

Table 1: Summary of the CDFW fish monitoring programs that provided data for abundance estimation. The number of sites sampled  $n$  has varied over time and the numbers shown are approximate. The analyzed column shows the years used in this study.

Survey	Duration	Analyzed	Frequency	Months	$n$
20-mm Survey (20-mm)	1995-present	1995-2017	Bi-weekly	Apr-Jul	60+
Summer Townet Survey (STN)	1959-present	1990-2017	Bi-weekly	Jun-Aug	30
Fall Midwater Trawl (FMWT)	1967-present	1990-2017	Monthly	Sep-Dec	100+
Spring Midwater Trawl (SMWT)	1990-2001	1991-2001	Monthly	Jan-May	100+
Spring Kodiak Trawl (SKT)	2002-present	2002-2017	Monthly	Jan-May	40+

Table 2: Delta Smelt abundance indices (standard errors in parentheses). NA denotes no available data for the given survey and year.

Year	20-mm	STN	FMWT	SMWT	SKT
1990	NA	944,890 (247,880)	485,426 (165,111)	NA	NA
1991	NA	3,947,36 (683,072)	1,178,446 (227,064)	131,260 (33,617)	NA
1992	NA	1,722,648 (287,981)	155,808 (57,644)	103,603 (26,762)	NA
1993	NA	7,957,836 (1,429,502)	1,861,967 (549,550)	55,630 (14,084)	NA
1994	NA	5,594,684 (743,458)	62,173 (24,175)	485,581 (106,027)	NA
1995	3,802,003 (1,714,167)	3,885,218 (503,118)	2,870,967 (541,800)	90,155 (24,314)	NA
1996	51,816,580 (9,680,651)	9,519,528 (3,741,334)	72,185 (24,425)	856,455 (205,410)	NA
1997	28,676,814 (5,422,401)	2,256,242 (650,399)	692,611 (204,958)	115,537 (27,425)	NA
1998	5,435,652 (2,523,076)	3,006,382 (558,410)	327,681 (70,380)	140,128 (41,206)	NA
1999	18,546,993(4,513,613)	9,307,496 (1,464,873)	2,198,820 (484,791)	171,469 (39,449)	NA
2000	24,333,860 (5,208,331)	6,029,290 (782,124)	717,813 (166,928)	539,175 (134,012)	NA
2001	19,761,621 (4,903,592)	4,940,657 (811,880)	2,059,595 (688,896)	245,506 (41,888)	NA
2002	5,330,964 (1,608,388)	2,441,040 (368,227)	345,150 (90,302)	NA	933,982 (225,097)
2003	6,661,403 (3,668,971)	1,546,580 (238,121)	833,943 (310,214)	NA	1,167,662 (165,504)
2004	11,334,053 (3,686,194)	696,211 (165,741)	451,505 (219,759)	NA	763,619 (161,573)
2005	13,754,192 (3,625,550)	1,139,543 (263,185)	64,973 (23,449)	NA	329,722 (101,264)
2006	3,360,377 (1,586,596)	590,540 (271,746)	33,479 (16,099)	NA	301,735 (45,389)
2007	1,659,962 (1,965,671)	311,681 (133,506)	23,371 (13,005)	NA	375,070 (124,451)
2008	1,427,033 (789,623)	508,404 (160,339)	53,864 (22,792)	NA	207,930 (82,196)
2009	5,190,179 (2,021,635)	285,517 (104,853)	23,970 (13,407)	NA	217,409 (72,908)
2010	4,870,088 (1,503,243)	1,170,651 (405,384)	43,910 (29,287)	NA	278,255 (90,568)
2011	4,205,030 (1,762,812)	3,589,513 (832,610)	279,154 (95,298)	NA	232,899 (83,947)
2012	16,626,279 (4,556,209)	611,230 (139,708)	112,339 (34,401)	NA	1,105,082 (388,559)
2013	5,379,031 (1,090,197)	715,704 (183,800)	20,975 (11,389)	NA	316,806 (93,219)
2014	1,868,430 (502,275)	266,270 (92,006)	11,781 (10,316)	NA	250,095 (80,597)
2015	525,597 (177,227)	3,201 (4,517)	2,886 (3,872)	NA	162,446 (74,258)
2016	426,070 (131,597)	11,676 (15,488)	19,348 (12,632)	NA	21,730 (8,901)
2017	690,469 (250,915)	320,293 (176,681)	7,502 (8,270)	NA	30,888 (9,561)

658 **Figure Captions**

659 Figure 1. Geographic stratification of the Delta into 29 subregions (geographic strata).

660 Figure 2. Abundance index time series, with vertical lines extending to +/- 1 standard error. Coef-  
661 ficient of variation is printed at the top. The vertical dashed grey line in the bottom panel separates  
662 adult abundance indices based on the SMWT survey (earlier years) from those based on the SKT  
663 (later years).

664 Figure 3. Abundance indices  $I_{l,s,y,m,g}$  computed here vs the CDFW indices, with points indicated  
665 by the last two digits of the calendar year of the data used in index construction. Dashed grey lines  
666 are regression through the origin predictions. Pearson pairwise complete correlations are shown in  
667 the top left of each panel.

668 Figure 4. Adult abundance indices (points) with vertical lines extending between the lower and  
669 upper confidence intervals for the years 2013-2017 based on the February and March SKT survey.  
670 The horizontal grey line is drawn at 55,000, above the upper confidence interval limits of 2016 and  
671 2017 and below the lower confidence interval limit for the years prior.

672 Figure 5. Proportion of the total variance of the abundance index by gear type for each of the three  
673 sources of variation: between sample location variation (source 1, solid lines), the randomness in  
674 catching fish that are available to the gear (source 2, dashed lines), and the uncertainty in the esti-  
675 mated probabilities of fish capture (source 3, dotted lines). SKT has the proportion from sampling  
676 location always 1 because the gear selectivity is assumed to be 1 with no uncertainty.



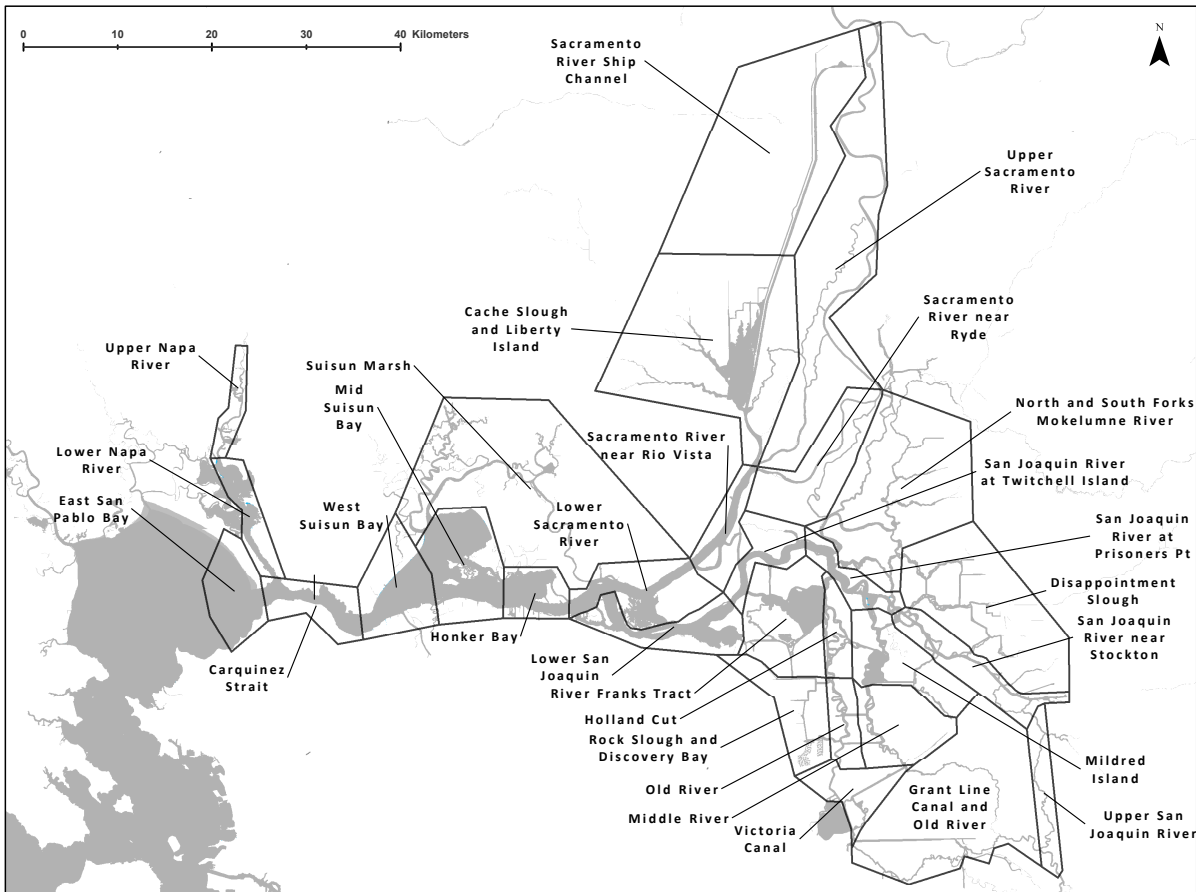


Figure 1: Geographic stratification of the Delta into 29 subregions (geographic strata)..

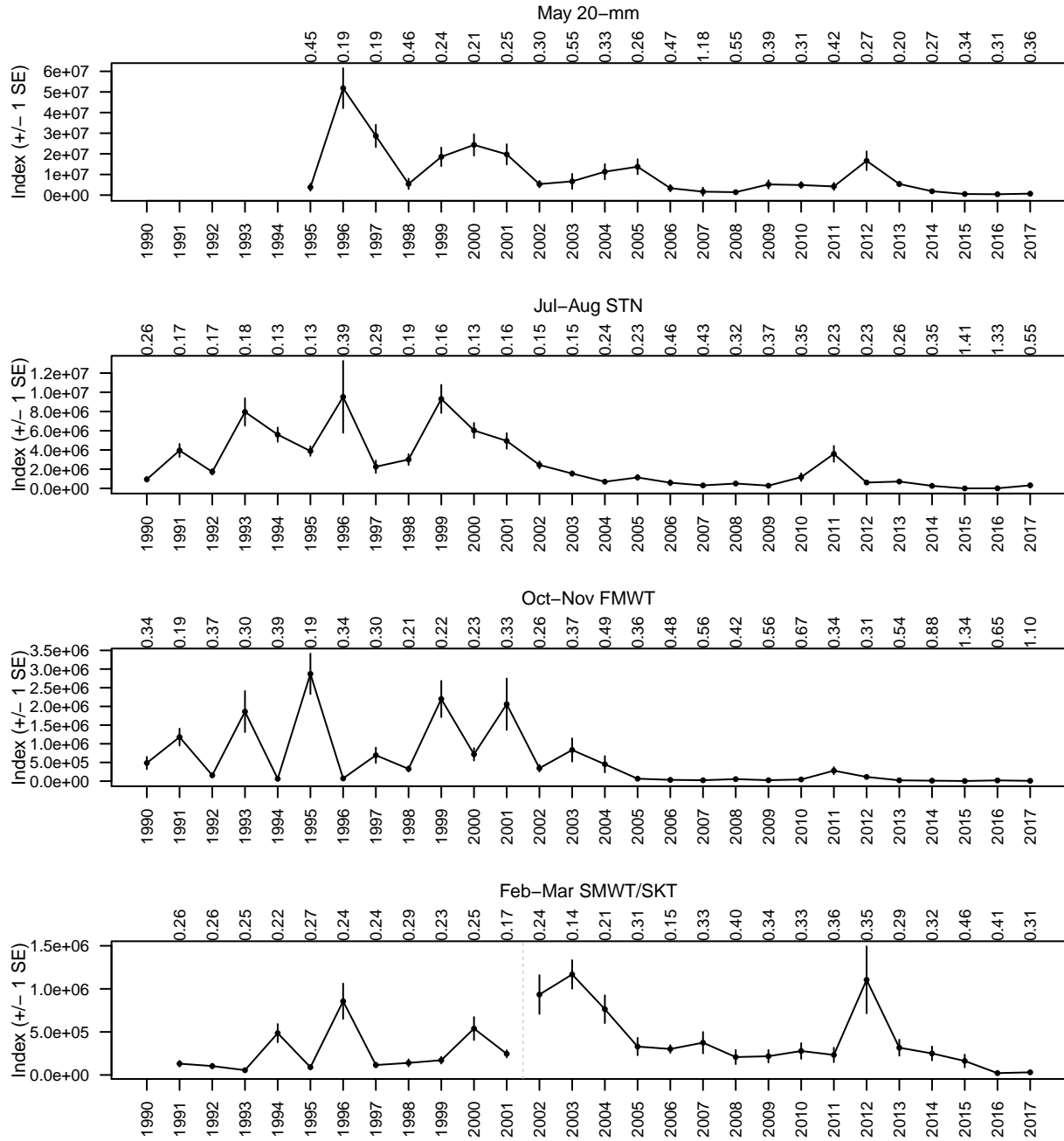


Figure 2: Abundance index time series, with vertical lines extending to +/- 1 standard error. Coefficient of variation is printed at the top. The vertical dashed grey line in the bottom panel separates adult abundance indices based on the SMWT survey (earlier years) from those based on the SKT (later years).

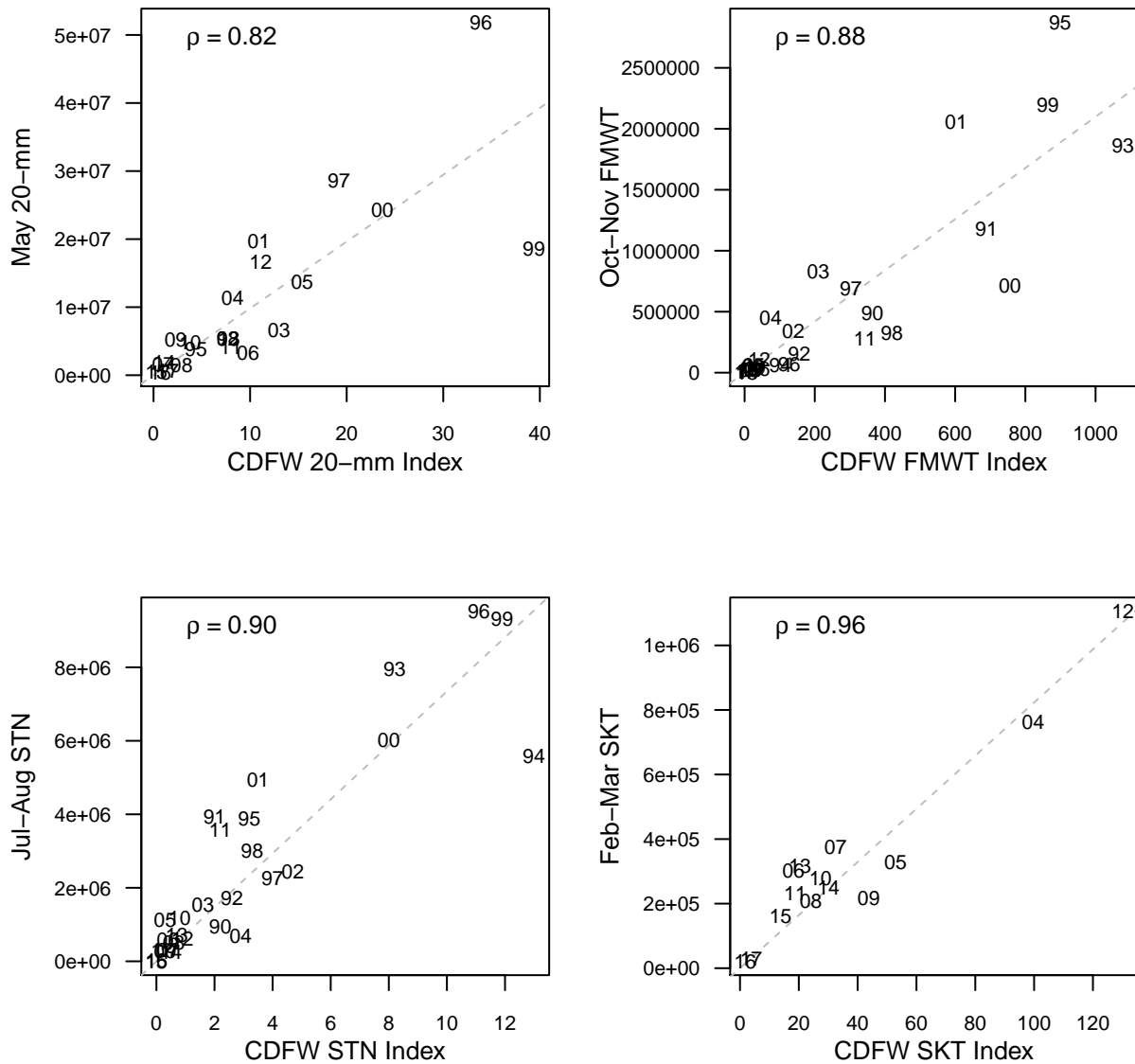


Figure 3: Abundance indices  $I_{l,s,y,m,g}$  computed here vs the CDFW indices, with points indicated by the last two digits of the calendar year of the data used in index construction. Dashed grey lines are regression through the origin predictions. Pearson pairwise complete correlations are shown in the top left of each panel.

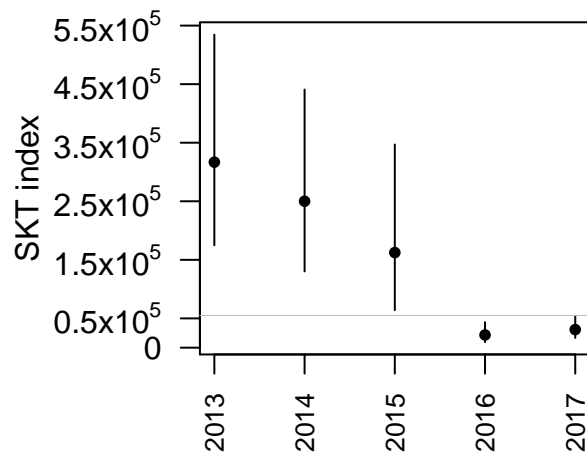


Figure 4: Adult abundance indices (points) with vertical lines extending between the lower and upper confidence intervals for the years 2013-2017 based on the February and March SKT survey. The horizontal grey line is drawn at 55,000, above the upper confidence interval limits of 2016 and 2017 and below the lower confidence interval limit for the years prior.

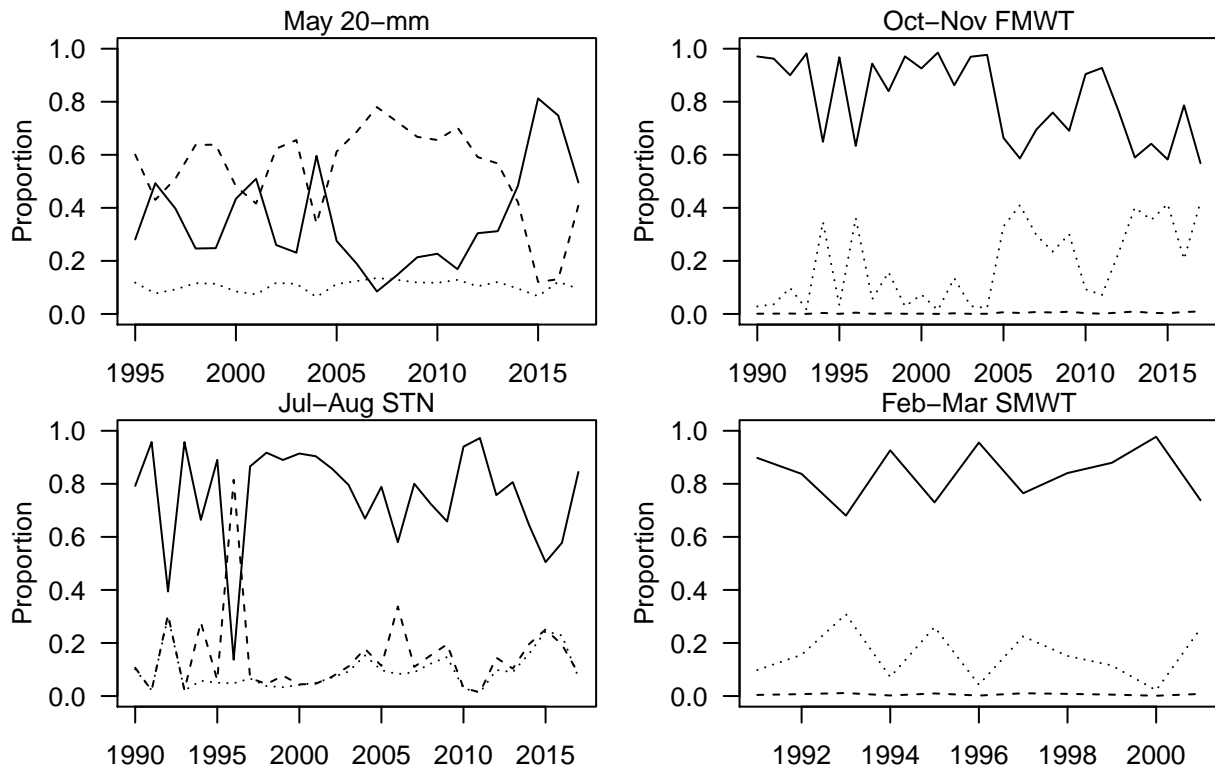


Figure 5: Proportion of the total variance of the abundance index by gear type for each of the three sources of variation: between sample location variation (source 1, solid lines), the randomness in catching fish that are available to the gear (source 2, dashed lines), and the uncertainty in the estimated probabilities of fish capture (source 3, dotted lines). SKT has the proportion from sampling location always 1 because the gear selectivity is assumed to be 1 with no uncertainty.

678 **Appendix A Variance of  $\hat{\delta}$**

679 The variance calculation that accounts for the three sources of uncertainty is similar to the formula  
 680 used for multistage sample designs (Hankin 1984; Newman 2008; Thompson 2002), which is  
 681 based on the law of total variance with three levels of variation. To reduce notation  $V$  and  $E$   
 682 correspond to variance and expected value respectively.

$$683 \quad V(\hat{\delta}) = E_1 \left[ E_2 \left( V_3(\hat{\delta}|1, 2) \right) \right] + E_1 \left[ V_2 \left( E_3(\hat{\delta}|1, 2) \right) \right] + V_1 \left[ E_2 \left( E_3(\hat{\delta}|1, 2) \right) \right] \quad (\text{A.1})$$

684 The sources of variation, labeled numerically, are (1) between sample location variation in the ratio  
 685 estimate of number of fish within a stratum, (2) the randomness in catching fish that are available  
 686 to the gear, and (3) uncertainty in the estimated probabilities of capture  $\hat{p}(L)$ .

687 The equation for  $\hat{\delta}$  is written below without subscripting for year, month, life stage, gear, and  
 688 stratum.

$$689 \quad \hat{\delta} = \frac{\sum_{j=1}^n \left( \sum_{i=1}^{c_j} \frac{1}{\hat{p}(L_i)} \right)}{\sum_{j=1}^n v_j^*}$$

690 Referring to Equation A.1, the innermost expectation and variance (at level 3, variance in the  
 691  $\hat{p}(L_i)$ ) refer to the estimated number of fish represented by the  $i$ th fish conditional on a known gear  
 692 selectivity function. The expectation and variance can be approximated as follows:

$$693 \quad E_3(\hat{\delta}|1, 2) \approx \frac{\sum_{j=1}^n \left( \sum_{i=1}^{c_j} \frac{1}{\hat{p}(L_i)} \right)}{\sum_{j=1}^n v_j^*} \quad (\text{A.2})$$

$$694 \quad V_3(\hat{\delta}|1, 2) = \frac{\sum_{j=1}^n \left( \sum_{i=1}^{c_j} V \left( \frac{1}{\hat{p}(L_i)} \right) \right)}{\left( \sum_{j=1}^n v_j^* \right)^2} \approx \frac{\sum_{j=1}^n \left( \sum_{i=1}^{c_j} \frac{1}{\hat{p}(L_i)^4} V(\hat{p}(L_i)) \right)}{\left( \sum_{j=1}^n v_j^* \right)^2} \quad (\text{A.3})$$

695 where the delta method is used to approximate the quantity  $V \left( \frac{1}{\hat{p}(L_i)} \right)$ .

697 The expectations and variances at the second level (variability in the number of fish caught) are

$$698 \quad E_2 \left( E_3(\hat{\delta}|1, 2) \right) = \frac{\sum_{j=1}^n E \left( \sum_{i=1}^{c_j} \frac{1}{p(L_i)} \right)}{\sum_{j=1}^n v_j^*} \approx \frac{\sum_{j=1}^n f_j}{\sum_{j=1}^n v_j^*} \quad (\text{A.4})$$

$$699 \quad V_2 \left( E_3(\hat{\delta}|1, 2) \right) \approx \frac{\sum_{j=1}^n V \left( \sum_{i=1}^{c_j} \frac{1}{p(L_i)} \right)}{\left( \sum_{j=1}^n v_j^* \right)^2} \approx \frac{\sum_{j=1}^n \left( \sum_{i=1}^{c_j} \frac{1-\hat{p}(L_i)}{\hat{p}(L_i)} \right)}{\left( \sum_{j=1}^n v_j^* \right)^2} \quad (\text{A.5})$$

$$700 \quad E_2 \left( V_3(\hat{\delta}|1, 2) \right) \approx \frac{\sum_{j=1}^n E \left( \sum_{i=1}^{c_j} \frac{1}{\hat{p}(L_i)^4} V(\hat{p}(L_i)) \right)}{\left( \sum_{j=1}^n v_j^* \right)^2} \approx \frac{\sum_{j=1}^n \left( \sum_{i=1}^{c_j^*} E[I_i] \frac{1}{\hat{p}(L_i)^4} V(\hat{p}(L_i)) \right)}{\left( \sum_{j=1}^n v_j^* \right)^2} \quad (\text{A.6})$$

$$701 \quad = \frac{\sum_{j=1}^n \left( \sum_{i=1}^{c_j^*} \frac{1}{\hat{p}(L_i)^3} V(\hat{p}(L_i)) \right)}{\left( \sum_{j=1}^n v_j^* \right)^2} \approx \frac{\sum_{j=1}^n \left( \sum_{i=1}^{c_j} \frac{1}{\hat{p}(L_i)^4} V(\hat{p}(L_i)) \right)}{\left( \sum_{j=1}^n v_j^* \right)^2} \quad (\text{A.7})$$

703 The term  $I_i$  on the right-hand side of Equation A.6 is an indicator variable for whether the  $i$ th fish  
 704 out of *all*  $c_j^*$  fish at site  $i$  is caught. It has an expected value of  $p(L_i)$  which cancels with one of the  
 705  $p(L_i)$  terms in the denominator yielding the first expression on the right-hand side of Equation A.7.

706 The total number of fish,  $c_i^*$ , and their respective lengths are unknown and that expression cannot  
 707 be calculated. However, the total number of fish of a given length  $L'$  can be estimated by  $c_{L'}/p(L')$   
 708 where  $c_{L'}$  is the observed number of length  $L'$  fish. This is the same as summing the  $1/p(L_i)$  over  
 709 the observed catch, thus  $1/p(L_i)$  is multiplied against  $\frac{1}{\hat{p}(L_i)^3} V(\hat{p}(L_i))$  yielding the final expression  
 710 in Equation A.7.

711 Lastly, expectations and variances are calculated at the first level.

$$712 \quad E_1 \left[ E_2 \left( V_3(\hat{\delta}|1, 2) \right) \right] \approx \frac{\sum_{j=1}^n \left( \sum_{i=1}^{c_j} \frac{1}{p(L_i)^4} V(\hat{p}(L_i)) \right)}{\left( \sum_{j=1}^n v_j^* \right)^2} \approx \frac{\sum_{j=1}^n \left( \sum_{i=1}^{c_j} \frac{1}{\hat{p}(L_i)^4} \hat{V}(\hat{p}(L_i)) \right)}{\left( \sum_{j=1}^n v_j^* \right)^2} \quad (\text{A.8})$$

$$713 \quad E_1 \left[ V_2 \left( E_3(\hat{\delta}|1, 2) \right) \right] \approx \frac{\sum_{j=1}^n \left( \sum_{i=1}^{c_j} \frac{1-p(L_i)}{p(L_i)} \right)}{\left( \sum_{j=1}^n v_j^* \right)^2} \approx \frac{\sum_{j=1}^n \left( \sum_{i=1}^{c_j} \frac{1-\hat{p}(L_i)}{\hat{p}(L_i)} \right)}{\left( \sum_{j=1}^n v_j^* \right)^2} \quad (\text{A.9})$$

$$714 \quad V_1 \left[ E_2 \left( E_3(\hat{\delta}|1, 2) \right) \right] \approx V_1 \left[ \frac{\sum_{j=1}^n f_j}{\sum_{j=1}^n v_j^*} \right] \approx \frac{\sum_{j=1}^n (c_j^* - \hat{\delta} v_j^*)^2}{v^{*2} n(n-1)} \quad (\text{A.10})$$

716

717 **Supplemental Materials: Using multistage design-based methods to construct abundance**  
718 **indices and uncertainty measures for Delta Smelt**

719 **A Subregion Water Volumes and Substitution Orders**

Table S1: Estimates of habitat volume, or volume of water occupied by Delta Smelt, by geographic stratum and fish stratum. Volumes are in cubic meters (m<sup>3</sup>).

Geographic stratum	Fish stratum	
	Later life stage (0.5 to 4.5 m)	Earlier life stage (0 to 10 m )
Cache Slough and Liberty Island	51,786,023	90,039,906
Carquinez Strait	60,455,559	135,019,878
Disappointment Slough	14,107,778	18,995,896
East San Pablo Bay	104,537,750	175,671,563
Franks Tract	52,701,925	71,232,869
Grant Line Canal and Old River	7,313,463	9,635,826
Holland Cut	17,642,507	27,809,216
Honker Bay	55,100,817	101,141,758
Lower Napa River	24,372,905	40,588,808
Lower Sacramento River	71,561,907	147,188,708
Lower San Joaquin River	76,919,425	141,250,258
Mid Suisun Bay	134,714,482	214,551,584
Middle River	9,000,880	13,707,843
Mildred Island	35,712,993	52,829,804
North and South Forks Mokelumne River	34,680,881	52,688,223
Old River	9,991,399	14,659,405
Rock Slough and Discovery Bay	3,718,423	4,718,521
Sacramento River near Rio Vista	45,878,622	83,461,347
Sacramento River near Ryde	12,833,585	18,948,518
Sacramento River Ship Channel	14,472,933	29,744,374
San Joaquin River at Prisoners Pt	36,436,501	67,727,034
San Joaquin River at Twitchell Island	32,369,636	66,601,478
San Joaquin River near Stockton	21,986,848	39,996,300
Suisun Marsh	30,289,939	47,763,576
Upper Napa River	800,061	1,733,454
Upper Sacramento River	37,840,015	57,161,007
Upper San Joaquin River	3,537,223	4,463,237
Victoria Canal	8,238,349	11,384,303
West Suisun Bay	89,106,803	172,557,863



Table S2: Percentage of habitat volume sampled by survey and month based on effective sample volumes.

Survey	Month	Mean	Min	Max
20-mm	May	0.012	0.008	0.017
20-mm	Jun	0.013	0.010	0.021
STN	Jun	0.008	0.004	0.018
STN	Jul	0.010	0.005	0.016
STN	Aug	0.008	0.002	0.015
STN	JulAug	0.016	0.005	0.026
FMWT	Sep	0.038	0.029	0.051
FMWT	Oct	0.040	0.034	0.051
FMWT	Nov	0.038	0.029	0.049
FMWT	Dec	0.037	0.030	0.046
FMWT	OctNov	0.077	0.063	0.100
SMWT	Jan	0.038	0.032	0.047
SMWT	Feb	0.039	0.031	0.053
SMWT	JanFeb	0.065	0.035	0.100
SMWT	JanFebMar	0.104	0.073	0.146
SMWT	FebMar	0.074	0.040	0.099
SKT	Jan	0.016	0.013	0.021
SKT	Feb	0.017	0.013	0.020
SKT	Mar	0.018	0.012	0.023
SKT	Apr	0.018	0.013	0.021
SKT	May	0.018	0.012	0.022
SKT	JanFeb	0.032	0.018	0.040
SKT	JanFebMar	0.049	0.040	0.061
SKT	FebMar	0.034	0.025	0.041

Table S3: List of subregion substitutions used in constructing abundance indices. The “Missing Subregion” is the subregion without data. Density and estimates from the first available “Substitute Subregion” were used as substitutes for the missing density. Abundance indices used the volume data of the missing subregion times density from the substitute region. Similarly, the variance of a missing subregion used the volume of that missing subregion.

Missing subregion	Substitute subregion
East San Pablo Bay	Carquinez Strait
East San Pablo Bay	Mid Suisun Bay
Upper Napa River	Lower Napa River
Upper Napa River	Carquinez Strait
Upper Napa River	West Suisun Bay
Upper Napa River	Mid Suisun Bay
Lower Napa River	Upper Napa River
Lower Napa River	Carquinez Strait
Lower Napa River	West Suisun Bay
Lower Napa River	Mid Suisun Bay
Carquinez Strait	West Suisun Bay
Carquinez Strait	East San Pablo Bay
Carquinez Strait	Lower Napa River
Carquinez Strait	Mid Suisun Bay
West Suisun Bay	Mid Suisun Bay
Mid Suisun Bay	West Suisun Bay
Suisun Marsh	Mid Suisun Bay
Suisun Marsh	Honker Bay
Suisun Marsh	Lower Sacramento River
Honker Bay	Mid Suisun Bay
Honker Bay	Suisun Marsh
Honker Bay	Lower Sacramento River
Lower Sacramento River	Lower San Joaquin River
Lower Sacramento River	Honker Bay
Lower Sacramento River	Suisun Marsh
Lower San Joaquin River	Suisun Marsh
Lower San Joaquin River	Lower Sacramento River
Lower San Joaquin River	Honker Bay
Sacramento River Ship Channel	Cache Slough and Liberty Island
Sacramento River Ship Channel	Upper Sacramento River
Sacramento River Ship Channel	Sacramento River near Ryde
Sacramento River Ship Channel	Sacramento River near Rio Vista
Sacramento River Ship Channel	San Joaquin River at Twitchell Island
Sacramento River near Rio Vista	Cache Slough and Liberty Island
Sacramento River near Rio Vista	San Joaquin River at Twitchell Island
Sacramento River near Ryde	Upper Sacramento River

Table S3 (continued)

Sacramento River near Ryde	Sacramento River near Rio Vista
Sacramento River near Ryde	Cache Slough and Liberty Island
Sacramento River near Ryde	San Joaquin River at Twitchell Island
Upper Sacramento River	Cache Slough and Liberty Island
Upper Sacramento River	Sacramento River near Ryde
Upper Sacramento River	Sacramento River near Rio Vista
Upper Sacramento River	San Joaquin River at Twitchell Island
Cache Slough and Liberty Island	Sacramento River Ship Channel
Cache Slough and Liberty Island	Lower San Joaquin River
Cache Slough and Liberty Island	San Joaquin River at Twitchell Island
Cache Slough and Liberty Island	Sacramento River near Rio Vista
San Joaquin River at Twitchell Island	Lower San Joaquin River
San Joaquin River at Twitchell Island	Cache Slough and Liberty Island
Franks Tract	Holland Cut
Franks Tract	San Joaquin River at Prisoners Pt
Franks Tract	San Joaquin River at Twitchell Island
North and South Forks Mokelumne River	San Joaquin River at Prisoners Pt
North and South Forks Mokelumne River	Sacramento River near Ryde
North and South Forks Mokelumne River	Upper Sacramento River
North and South Forks Mokelumne River	Disappointment Slough
San Joaquin River at Prisoners Pt	Holland Cut
San Joaquin River at Prisoners Pt	Middle River
San Joaquin River at Prisoners Pt	Old River
San Joaquin River at Prisoners Pt	Mildred Island
Holland Cut	San Joaquin River at Prisoners Pt
Holland Cut	Middle River
Holland Cut	Old River
Holland Cut	Mildred Island
Middle River	Mildred Island
Middle River	Old River
Middle River	Holland Cut
Middle River	San Joaquin River at Prisoners Pt
Upper San Joaquin River	San Joaquin River near Stockton
Upper San Joaquin River	Disappointment Slough
Upper San Joaquin River	Middle River
Upper San Joaquin River	Mildred Island
Upper San Joaquin River	North and South Forks Mokelumne River
Upper San Joaquin River	Sacramento River near Ryde
Victoria Canal	Old River
Victoria Canal	Middle River
Victoria Canal	Grant Line Canal and Old River

Table S3 (continued)

Victoria Canal	San Joaquin River near Stockton
Victoria Canal	Rock Slough and Discovery Bay
Grant Line Canal and Old River	Victoria Canal
Grant Line Canal and Old River	Middle River
Grant Line Canal and Old River	Old River
Grant Line Canal and Old River	San Joaquin River near Stockton
Grant Line Canal and Old River	Rock Slough and Discovery Bay
San Joaquin River near Stockton	Victoria Canal
San Joaquin River near Stockton	Grant Line Canal and Old River
San Joaquin River near Stockton	Rock Slough and Discovery Bay
Disappointment Slough	North and South Forks Mokelumne River
Disappointment Slough	Upper San Joaquin River
Disappointment Slough	San Joaquin River at Prisoners Pt
Disappointment Slough	Sacramento River near Ryde
Rock Slough and Discovery Bay	Old River
Rock Slough and Discovery Bay	Victoria Canal
Rock Slough and Discovery Bay	Holland Cut
Rock Slough and Discovery Bay	Grant Line Canal and Old River
Rock Slough and Discovery Bay	San Joaquin River near Stockton
Old River	Holland Cut
Old River	Franks Tract
Old River	Mildred Island
Old River	San Joaquin River at Prisoners Pt
Old River	Middle River
Mildred Island	Old River
Mildred Island	Middle River
Mildred Island	Holland Cut
Mildred Island	San Joaquin River at Prisoners Pt
Mildred Island	Franks Tract

---

720 **B Survey Station Locations**

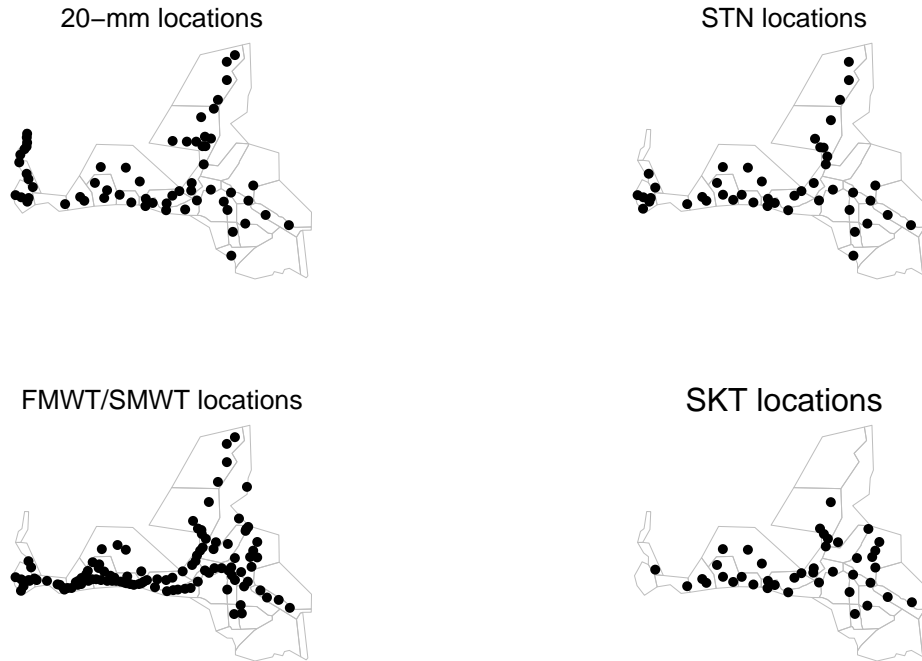


Figure S1: Station locations for each survey.

721 **C Data Processing**

722 This section provides a brief overview of the data sets used to calculate design-based estimates.  
723 We started with survey-specific files containing catch and length data provided by CDFW. The  
724 20-mm and SKT surveys periodically conduct investigative or experimental surveys; we removed  
725 data from these supplemental surveys and retained data from routine surveys, which correspond  
726 to annual survey numbers 1 through 5 for SKT and 1 through 9 for 20-mm. Each survey program  
727 (20-mm, STN, FMWT, SKT) has core stations that have been sampled since the beginning of the  
728 survey as well as non-core stations that have been consistently sampled starting in more recent  
729 years. We retained data from both core and non-core stations. We also retained stations that were  
730 sampled sporadically but were not part of a complete supplemental survey.

731 We imputed missing or physically unrealistic values of tow volume (i.e., volume of water sampled  
732 in a tow), station depth (i.e., depth to the bottom of the sampling location), and “cable out”, which  
733 is the amount of cable let out when conducting an oblique tow (see section “Sample volume ad-  
734 justments”). Mean values, calculated at the finest spatiotemporal resolution possible, were used as  
735 substitute values. The finest resolution we considered for these variables was date-station. We also  
736 imputed fork lengths for Delta Smelt that were not measured for length. If other Delta Smelt were  
737 caught and measured in the same tow, we used the mean fork length from that tow, otherwise we  
738 used the mean fork length calculated for a given year-survey number combination or for a given  
739 month (calculated across years), if necessary.

740 Some of the tow depth values that were calculated as described in the section “Sample volume  
741 adjustments” were physically unrealistic and in these cases we replaced the unrealistic values as  
742 follows. If a calculated tow depth was greater than station depth, we replaced the calculated tow  
743 depth with station depth. When cable out values are at the low end of the range (e.g., 75 feet), the  
744 corresponding tow depth can be less than the mouth height of the net. If the net does break the  
745 surface of the water during sampling, the crew will slow the boat and increase the cable angle to  
746 keep the net fully submerged (T. Morris, personal communication, February 23, 2016). As a result,  
747 if a calculated tow depth was less than the mouth height, we replaced the calculated tow depth with  
748 the mouth height.

#### 749 **D Organization of R Code and Output**

750 Accompanying this document are input data and R (R Foundation for Statistical Computing, Vi-  
751 enna, Austria) code needed to run this analysis. They are contained in the directory `code_and_data`.

752 Everything can be run from the file `run_vX.r`, where `vX` denotes a version number. The file  
753 `DataCleaner_FishSurveys_vX.r` does the initial data processing and the file `Design_based_abund.ca`  
754 which depends on the file `Abund_util_vX.r`, calculates the design-based abundance indices.

755 This analysis produces three csv files and one RData file:

756 DB\_abundance\_long\_vX\_DATE.csv

757 DB\_abundance\_wide\_vX\_DATE.csv

758 DB\_abundance\_wide\_cohort\_vX\_DATE.csv

759 Design\_based\_abund\_calc\_vX\_DATE\_Everything.RData

760 where vX represents the version number from the Design\_based\_abund\_calc\_vX.r script  
761 and DATE represents the date on which the file was generated. The csv files contain the same data  
762 but are organized differently. The first has a separate record for each combination of calendar year,  
763 month, gear type, and Delta Smelt age class. The second has a separate row for each calendar year  
764 and different columns for different combinations of survey type, month, and age class. The third  
765 file is similar to the second file except that each row corresponds to a different cohort year, where a  
766 cohort year is defined roughly from March of the year the cohort was born to June of the following  
767 year. The .RData is a copy of the R workspace after all objects are loaded in and the calculations  
768 are executed.

769 **E Simulation Study to Evaluate the Use of a Lognormal Distribution in Abundance Ap-**  
770 **proximation**

771 Catch data and indice estimates were simulated under different scenarios of gear selectivity curves.  
772 An adjustment related to the use of effective volume was not included because this is not treated  
773 as a source of variability in the estimation process. Further, availability was assumed to be 100%  
774 thus total abundances, not just indices, were estimated.

775 Fish lengths were scaled to lie between 0 and 1. Nine different selectivity curves, intended to  
776 cover a wide range of possible gear efficiencies and dependencies (or the near lack of) on fish  
777 length, were used to simulate catch (Figure S2). The pseudo-code in Box E1 describes how catch  
778 abundances were simulated, and parameter values shown in Table S4. These values were selected  
779 to approximate the Delta Smelt survey efforts and data. For the choice of  $H$ ,  $V_h$ , and  $\delta_h$ , the  
780 simulated baseline abundance was  $N = 102,000$  (5,100 per each of the 20 strata).

781 A total of 1,000 simulations for each gear selectivity choice were made. The distributions were  
782 right-skewed with the degree of skewness varying as a function of the contact selectivity parameters  
783 (Figure S3). Estimates of  $N_{Tot}$  equal to zero resulted only for the selectivity curves closest to zero  
784 across much of the range of fish lengths (e.g.,  $\beta_0=0.9$  and  $\beta_1=10$ , Table S7). The bias was relatively  
785 low, ranging from -1.7% to 2.2% (Table S5). The coefficient of variation could be relatively large,  
786 ranging from 37% to 91% (Table S6). Actual coverage of the 95% confidence intervals based on  
787 the lognormal distribution was affected by the contact selectivity function with exact coverage for  
788 the mid-range intercept ( $\beta_0=0.5$ ), slightly low for the negative intercept ( $\beta_0 = -0.5$ ), and too high  
789 (97 to 100%) for the largest intercept ( $\beta_0=0.9$ , Table S4). On the other hand, confidence intervals  
790 based on a normal distribution yielded negative lower bounds with increasing probability as  $\beta_0$   
791 increased (Table S4).



**Box E1: Pseudo-code to simulate indice estimates**

- (1) Choose a total number of strata  $H$  and stratum specific densities  $\delta_h$  with which to set the simulated baseline abundances  $N_h$  and total  $N_{Tot} = \sum_h N_h$ .
- (2) For  $h$  in  $1, \dots, H$
- (i) For  $j$  in  $1, \dots, n_{h,j}$
- (a) Simulate the baseline abundance in the sampled volume of water  $v_s$  according to a negative binomial distribution,  $y_{h,j} \sim \text{NegBin}(\mu = \delta_h * v_s, \theta)$ . This simulates random *potential* catch level variation.
- (b) If  $y_{h,j} > 0$
- A. Assign lengths to each of the  $y_{h,j}$  fish in the patch of water sampled according to a length distribution,  $L_{h,j,i} \sim \text{Beta}(\alpha_1, \alpha_2)$ .
- B. For  $i$  in  $1, \dots, y_{h,j}$  simulate a Bernoulli random variable  $I_{h,j,i} \sim \text{Bern}(p = p_g(L_{h,j,i}))$  and assign these fish to the total catch  $c_{h,j} = \sum_i I_{h,j,i}$ . This step simulates a random total catch according to the gear selectivity function,  $p_g(L)$ , which was modeled with a logit transform:  $\text{logit}(p_g(L)) = \beta_1(L - \beta_0)$ . The lengths of the specific fish assigned to the total catch are recorded.
- C. Compute the adjusted catch  $c_{h,j}^* = \sum_i^{c_{h,j}} 1/p_g(L_{h,j,i})$ .
- (ii) Compute the estimated stratum density as a ratio of means,  $\hat{\delta}_h = \frac{\sum_j^{n_{h,j}} c_{h,j}^*}{\sum_j^{n_{h,j}} v_{s,j}}$ .
- (iii) Compute the estimated stratum total  $\hat{N}_h = \hat{\delta}_h V_h$  and the estimated variance  $\widehat{\text{Var}}(\hat{N}_h)$  according to Appendix A.
- (3) Estimate the total abundance  $\hat{N}_{Tot} = \sum_h \hat{N}_h$  and total variance  $\widehat{\text{Var}}(\hat{N}_{Tot}) = \sum_h \widehat{\text{Var}}\hat{N}_h$ .
- (4) Use the total abundance and total variance estimates to parameterize normal and lognormal distributions for confidence interval construction, check to see if  $N_{Tot}$  falls within the confidence intervals, check if the lower confidence intervals based on a normal distribution are negative, and compute other summary statistics.

Table S4: Parameter values used for the simulation study.

Parameter	Value	Description
$V_h$	$5.1 \times 10^7 \text{m}^3$	Stratum volume, a constant.
$\delta$	$0.005 \text{ fish/m}^3$	True density in each stratum.
$\theta$	0.2	Dispersion parameter for the negative binomial distribution used to simulate stratum values. Parameterized so that $\text{Var}(y_{h,j}) = \delta * v_s + (\delta * v_s)^2 / \theta$ .
$v_s$	$10,000 \text{m}^3$	Sample volume.
$H$	20	Total number of strata.
$n_{h,j}$	3	Number of replicate samples per stratum.
$\alpha_1 (= \alpha_2)$	60	Shape parameters for the beta distribution assigning lengths to the fish in each stratum. The expected length of the fish in each stratum is 0.5 and the variance is $\alpha_1 \alpha_2 / ((\alpha_1 + \alpha_2)^2 (\alpha_1 + \alpha_2 + 1))$ .
$\beta_0$	-0.5, 0.5, 0.9	Mid-point parameter for the selectivity function $p_g(L)$ , the length at which an individual has a 0.5 probability of being captured. Negative values have the effect of making fish (with lengths between 0 and 1) have a high and nearly constant value of being captured. See Figure S2.
$\beta_1$	1, 5, 10	Slope parameter of the selectivity function $p_g(L)$ . See Figure S2.
$\text{Var}(\hat{p}_g(L))$	0.07	Variance of the selectivity curve estimate. This was made constant across fish lengths and chosen from the larger values of the empirically estimated ones.

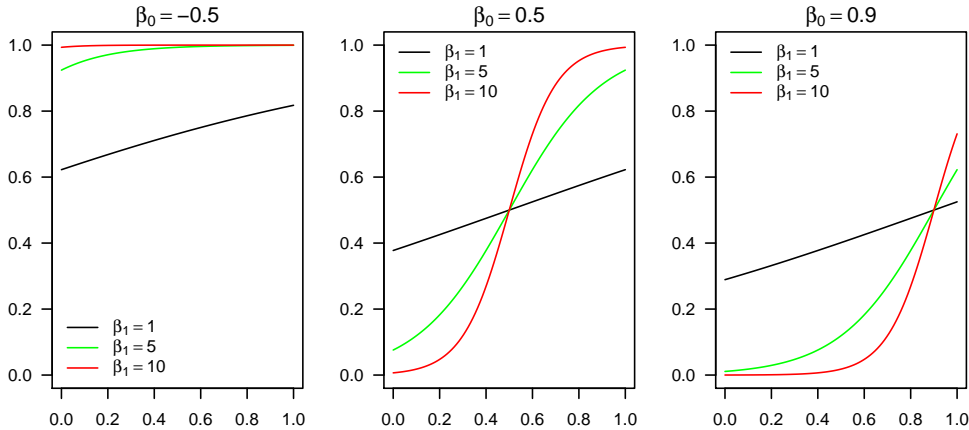


Figure S2: Selectivity curves,  $p_g(L)$ , used in the simulation study. Lengths (between 0 and 1) are on the x-axis and the probability of capture is on the y-axis. The mid-point parameter value is printed above each panel, with three different slope parameter values used per mid-point parameter value.

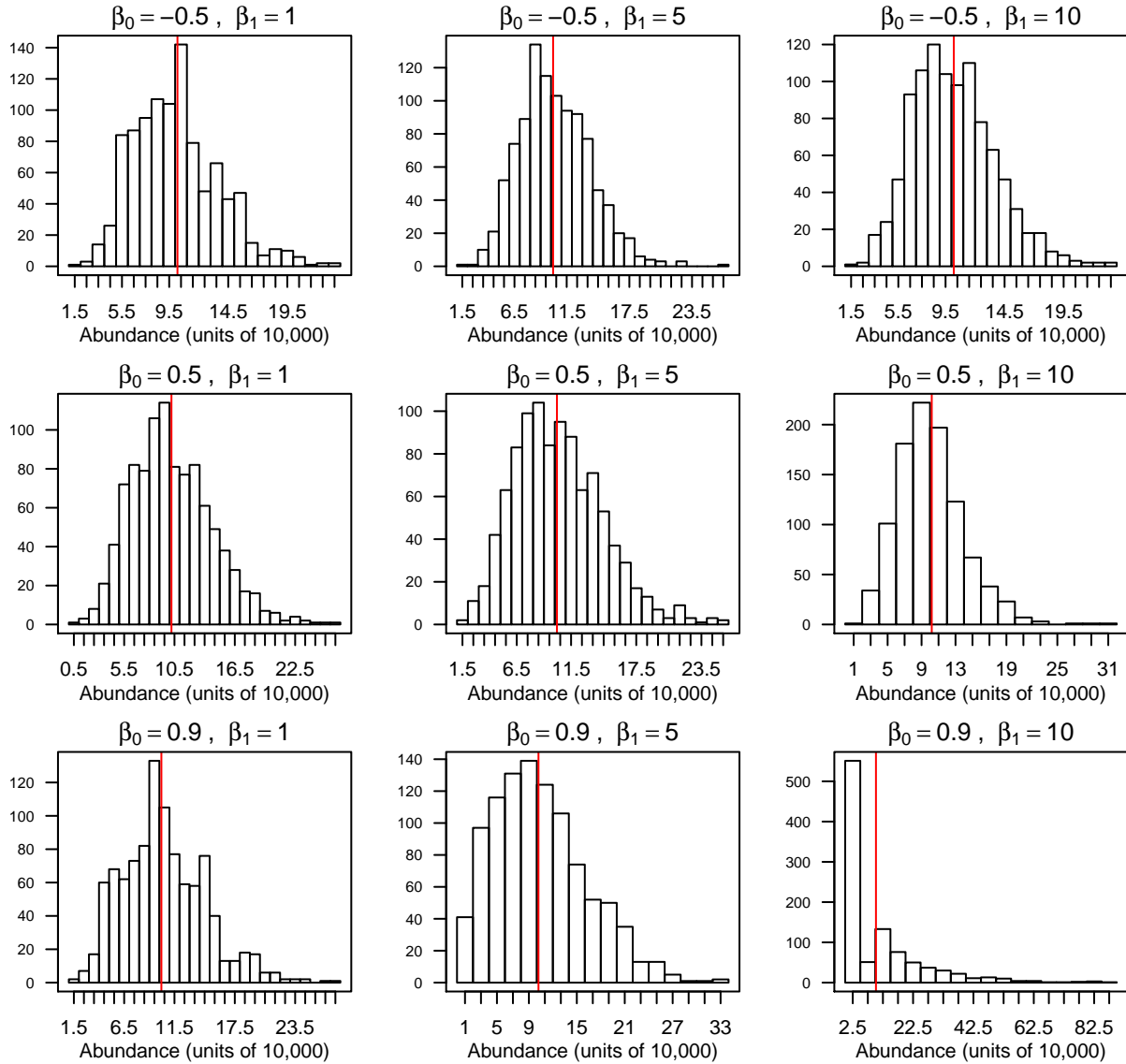


Figure S3: Histograms of abundance point estimates  $\hat{N}_{Tot}$  from 1,000 simulations based on the nine different selectivity curves. The red lines are drawn at the value of the baseline total  $N_{Tot}$ .

Table S5: Relative percent bias of  $\hat{N}_{Tot}$  ( $(\hat{N}_{Tot} - N_{Tot})/N_{Tot} * 100$ ) by gear selectivity curve.

	$\beta_1 = 1$	$\beta_1 = 5$	$\beta_1 = 10$
$\beta_0 = -0.5$	-1.39	0.67	-1.67
$\beta_0 = 0.5$	0.25	1.08	-1.42
$\beta_0 = 0.9$	2.21	1.29	-1.44

Table S6: Mean coefficient of variation of those estimates with nonzero point estimates, i.e., those which had at least one nonzero adjusted catch value; see Table S7 for the proportions of simulations with abundance indices of zero.

	$\beta_1 = 1$	$\beta_1 = 5$	$\beta_1 = 10$
$\beta_0 = -0.5$	0.41	0.37	0.40
$\beta_0 = 0.5$	0.48	0.47	0.46
$\beta_0 = 0.9$	0.47	0.79	0.91

Table S7: Proportion of the simulations with zero abundance index (i.e., the proportion of times that no fish were caught in 60 tows).

	$\beta_1 = 1$	$\beta_1 = 5$	$\beta_1 = 10$
$\beta_0 = -0.5$	0	0	0
$\beta_0 = 0.5$	0	0	0
$\beta_0 = 0.9$	0	0.03	0.55

793 **F The Effect of Truncation**

Table S8: Ratios of non-truncated abundance to truncated abundance by survey and time period of data collection. Missing entries correspond to time periods during which no data were collected.

Year	20-mm		STN			
	May	June	June	July	August	July-August
1995	1.20	2.00		1.25	1.25	1.50
1996	1.07	1.96		1.34	1.34	1.34
1997	1.18	3.83	1.21	1.53	1.53	1.53
1998	1.04	3.44		1.58	1.58	1.66
1999	1.13	1.57		1.35	1.35	1.38
2000	1.06	2.67	1.08	1.38	1.38	1.42
2001	1.11	3.68	1.10	1.39	1.39	1.39
2002	1.27	6.94	1.26	1.37	1.37	1.49
2003	1.07	1.84	1.06	1.49	1.49	1.64
2004	1.26	4.97	1.23	1.52	1.52	1.66
2005	1.15	5.55	1.22	1.58	1.58	1.71
2006	1.10	2.65	1.14	1.21	1.21	1.23
2007	1.05	5.58	1.21	1.62	1.62	1.70
2008	1.63	10.27	1.18	1.67	1.67	1.81
2009	1.20	3.87	1.34	1.60	1.60	1.92
2010	1.30	3.08	1.45	1.70	1.70	1.76
2011	1.15	1.53	1.04	1.26	1.26	1.31
2012	1.06	1.54	1.07	1.26	1.26	1.33
2013	1.50	4.08	1.18	1.79	1.79	1.81
2014	1.81	6.05	1.18	1.70	1.70	1.79
2015	2.43	5.34	1.60			1.95
2016	2.10	10.47	1.40			1.67
2017	1.60	7.76	1.82	1.56	1.56	1.81

Table S9: Pearson correlations between non-truncated and truncated abundance indices using pairwise complete observations.

20-mm		STN			
May	June	June	July	August	July-August
1.00	0.90	1.00	1.00	1.00	1.00

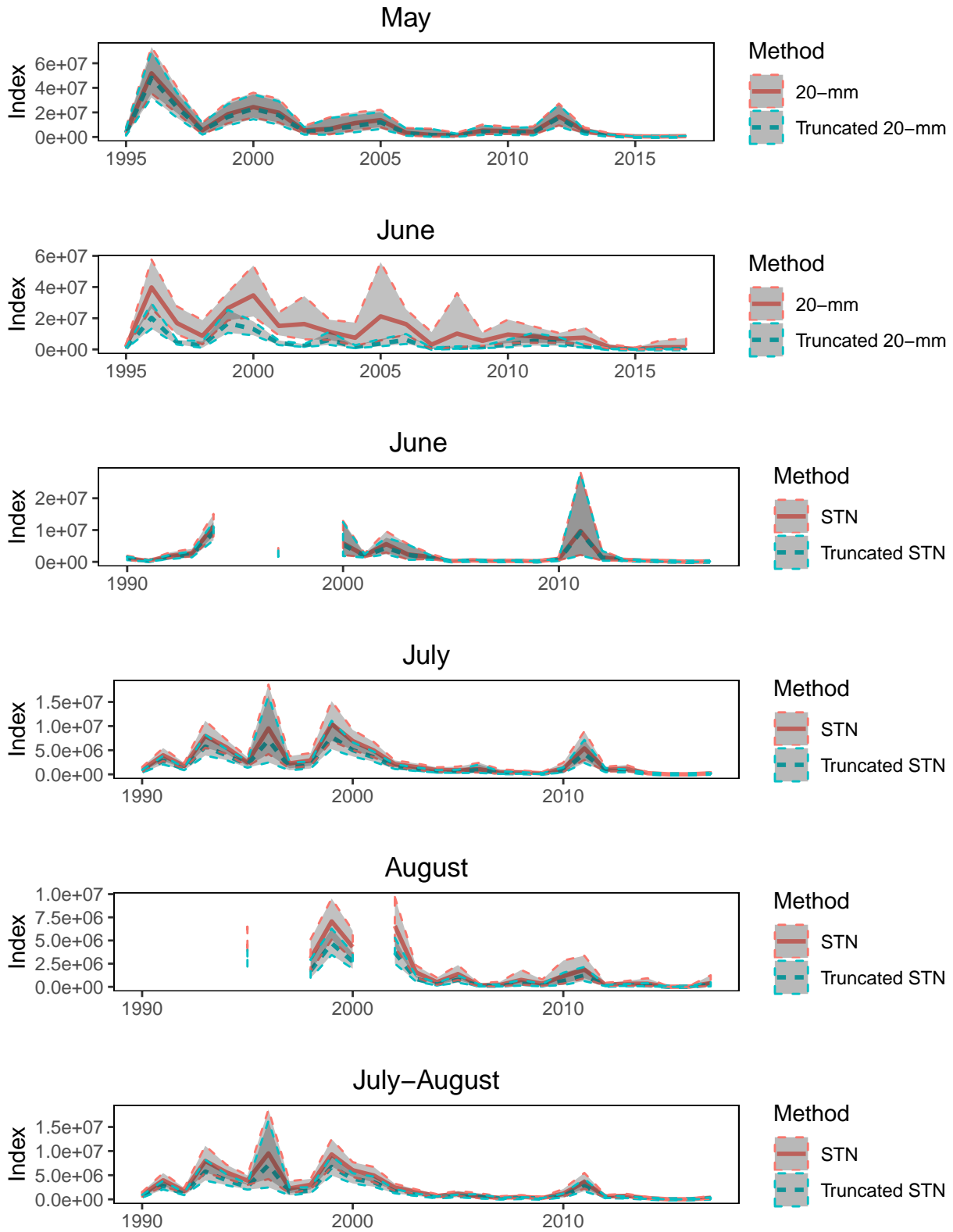


Figure S4: Abundance time series plots and 95 confidence envelopes based on non-truncated and truncated selectivity curves.

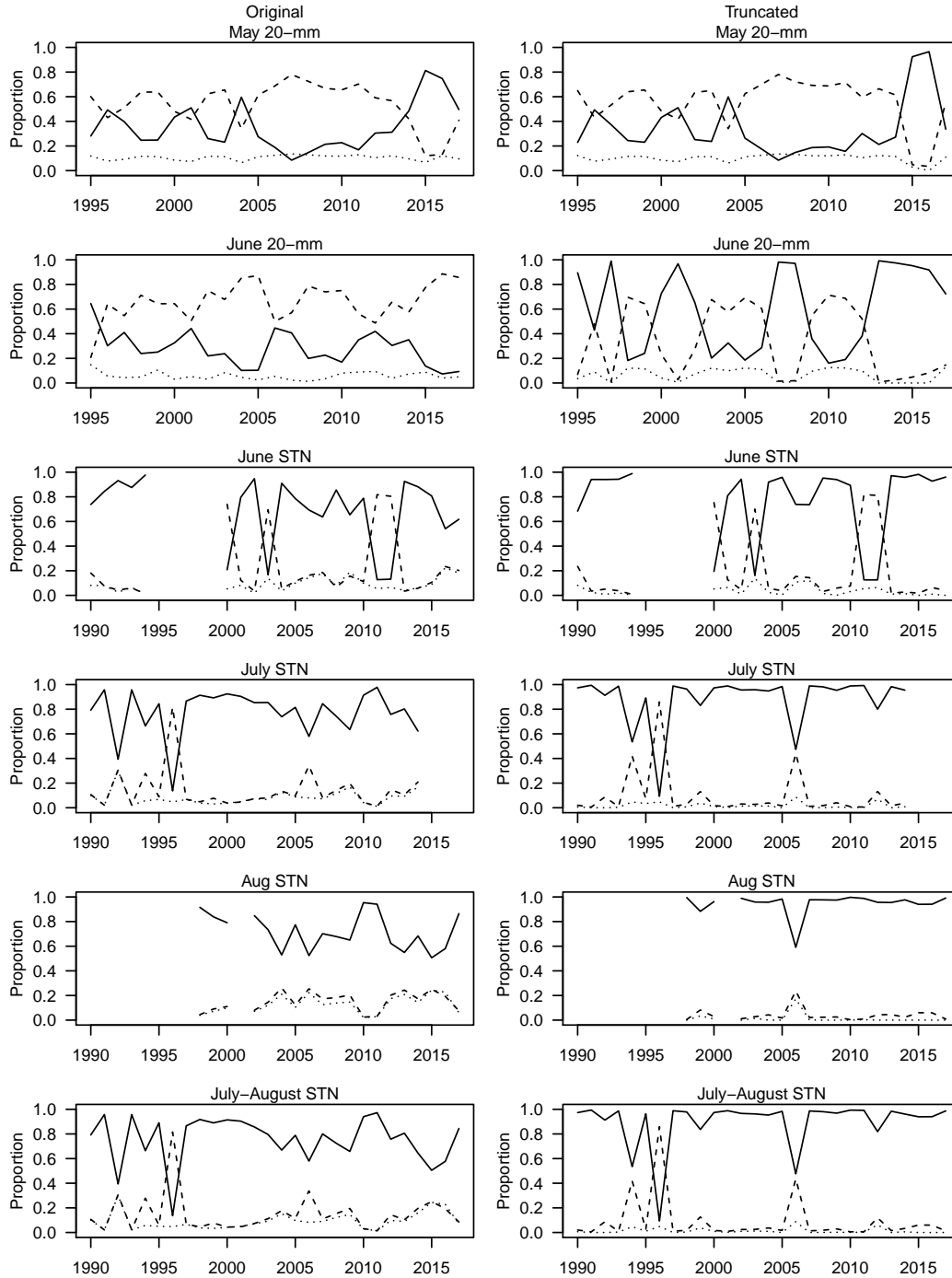


Figure S5: Proportion of the total variance of the estimated population abundance by gear type and non-truncated and truncated based catch adjustments for each of the three sources of variation: between sample variation (source 1, solid lines), the randomness that a fish present in the tow volume will be caught (source 2, dashed lines), and the variability in the estimate of selectivity curve (source 3, dotted lines). For ease of comparison the non-truncated figures are repeated here as well as in the main text (compare with Figure 5).